



Published in final edited form as:

J Med Chem. 2012 May 24; 55(10): 4847–4860. doi:10.1021/jm300396n.

Structure-Guided Design of A₃ Adenosine Receptor-Selective Nucleosides: Combination of 2-Arylethynyl and Bicyclo[3.1.0]hexane Substitutions

Dilip K. Tosh^{a,c}, Francesca Deflorian^{a,c}, Khai Phan^a, Zhan-Guo Gao^a, Tina C. Wan^b, Elizabeth Gizewski^b, John A. Auchampach^b, and Kenneth A. Jacobson^{a,*}

^aMolecular Recognition Section, Laboratory of Bioorganic Chemistry, National Institute of Diabetes and Digestive and Kidney Diseases, National Institutes of Health, Bethesda, Maryland 20892

^bDepartment of Pharmacology, Medical College of Wisconsin, 8701 Watertown Plank Road, Milwaukee, WI 53226

Abstract

(N)-Methanocarba adenosine 5'-methyluronamides containing known A₃ AR (adenosine receptor)-enhancing modifications, i.e. 2-(arylethynyl)adenine and N⁶-methyl or N⁶-(3-substituted-benzyl), were nanomolar full agonists of human (h) A₃AR and highly selective (K_i ~0.6 nM, N⁶-methyl 2-(halophenylethynyl) analogues **13**, **14**). Combined 2-arylethynyl-N⁶-3-chlorobenzyl substitutions preserved A₃AR affinity/selectivity in the (N)-methanocarba series (e.g. 3,4-difluoro full agonist MRS5698 **31**, K_i 3 nM, human and mouse A₃) better than for ribosides. Polyaromatic 2-ethynyl N⁶-3-chlorobenzyl analogues, such as potent linearly extended 2-*p*-biphenylethynyl MRS5679 **34** (K_i hA₃ 3.1 nM; A₁, A_{2A}: inactive) and fluorescent 1-pyrene adduct MRS5704 **35** (K_i hA₃ 68.3 nM) were conformationally rigid; receptor docking identified a large, mainly hydrophobic binding region. The vicinity of receptor-bound C2 groups was probed by homology modeling based on recent X-ray structure of an agonist-bound A_{2A}AR, with a predicted helical rearrangement requiring an agonist-specific outward displacement of TM2 resembling opsin. Thus, X-ray structure of related A_{2A}AR is useful in guiding design of new A₃AR agonists.

Keywords

G protein-coupled receptor; purines; molecular modeling; structure activity relationship; radioligand binding; adenylate cyclase

Introduction

The structure activity relationship (SAR) of nucleoside agonists at the A₃ adenosine receptor (AR), a G protein-coupled receptor (GPCR) of the rhodopsin-like family A, has been extensively explored.¹ Several A₃AR-selective agonists are currently in advanced clinical

*Corresponding author: kajacobs@helix.nih.gov, Molecular Recognition Section, Bldg. 8A, Rm. B1A-19, NIH, NIDDK, LBC, Bethesda, MD 20892-0810, Tel.: 301-496-9024, Fax: 301-480-8422.

^ccontributed equally to this work.

Supporting information available:

Docking figures for compounds **14**, **15** and **34**, procedures for synthesis of intermediates, detailed molecular modeling procedures, and biological assays for novel nucleoside derivatives, and coordinates of complexes with **13**, **31** and **35**. This material is available free of charge via the Internet at <http://pubs.acs.org>.

The synthetic route used to prepare (N)-methanocarba 5'-*N*-methyluronamido derivatives containing a 2-arylethynyl group involved a key Sonogashira reaction²⁷ at a 2-iodoadenine moiety of intermediate **43** or **44** (Scheme 1). L-Ribose **38** was converted as previously reported into the 2',3'-protected intermediate **39** containing a 5-ethyl ester, which was then subjected to a Mitsunobu condensation with 2-iodo-6-chloropurine to give **40**.^{21,28} A *N*⁶-methyl or *N*⁶-(3-chlorobenzyl) group was added by nucleophilic substitution of 6-chloro at room temperature to provide intermediates **41** and **42**, respectively, followed by aminolysis of the ester at room temperature leading to 5'-*N*-methyluronamides **43** and **44**. A Sonogashira reaction was then carried out with a variety of commercially available arylacetylenes to give protected nucleosides **45** – **46** (*N*⁶-methyl) and **47a** - **f** (*N*⁶-3-chlorobenzyl). Finally, acid hydrolysis of the isopropylidene protecting group provided *N*⁶-methyl **9** – **26** and *N*⁶-3-chlorobenzyl **27** – **36** nucleosides. The associated synthesis of a polyaromatic ethynyl intermediate **51** is shown in Scheme 2.

Pharmacological activity

Radioligand binding assays at three hAR subtypes were carried out using standard ³H (**52**, **53**) and ¹²⁵I-labeled (**54**) nucleosides (Table 1).^{29–31} The membrane preparations were obtained from Chinese hamster ovary (CHO) cells (A₁ and A₃) or human embryonic kidney (HEK293) cells (A_{2A}) stably expressing a hAR subtype.^{28,29,32,33} A₃AR binding curves generally showed a Hill coefficient of ~1. The nucleoside analogues were not screened for activity at the hA_{2B}AR, because other (N)-methanocarba nucleosides were previously noted to be very weak or inactive at that subtype.¹⁵ For example, in cyclic AMP assays, agonist **3** displayed 30,000-fold selectivity for the hA₃AR in comparison to the hA_{2B}AR.¹⁷ Some previously reported 2-chloro and 2-alkynyl (N)-methanocarba agonists (**3** – **8**) were used for comparison in the biological assays.²⁰ For exploring species differences in AR ligand recognition, binding assays were also performed on selected nucleoside derivatives at three mouse (m) ARs (Table 2) expressed in HEK293 cells.^{21,33b}

The simplest *N*⁶-methyl 2-phenylethynyl analogue **9** displayed a subnanomolar K_i value at the hA₃AR and was nearly inactive at the hA₁AR and hA_{2A}AR, with <20% inhibition of binding at 10 μM. Therefore, the degree of A₃AR selectivity of **9** was estimated to be >10,000-fold. The effects of phenyl modification of the C2-arylethynyl group at the C2 position were explored initially in the *N*⁶-methyl 5'-*N*-methyluronamide series. These derivatives displayed great freedom of substitution of the arylethynyl moiety, i.e. aza substitution of a CH of phenyl (**10**), monohalo (**11** – **17**) and dihalo (**19**, **20**) or other (**18**, **21** – **23**) substituent groups on the phenyl ring, and the presence of additional aryl rings (**24** – **26**). The 3,4-difluorophenyl analogue **19** was particularly A₃AR-selective with insignificant inhibition at A₁ and A_{2A}ARs. Planar polyaromatic groups, such as α-naphthyl **25** and the larger phenanthrene **26**, in the *N*⁶-methyl series did not interfere with the binding to the hA₃AR. The presence of a branched *p*-*t*-Bu group in **22** reduced A₃AR binding affinity by 12-fold compared to the H analogue **9**. The most potent A₃AR ligands in the *N*⁶-methyl series were halo-substituted compounds **13** and **14** with K_i values of 0.5 – 0.6 nM. A *p*-acetyl substitution in **23** was lower in hA₃AR affinity and higher in hA_{2A}AR affinity than most other ring substitutions, unlike in the riboside series of Cristalli and coworkers,^{23a} in which a 2(-*p*-acetylphenylethynyl) group favored A₃AR affinity and selectivity.

The variability of binding affinity upon substitution of the arylethynyl moiety was greater at the hA_{2A}AR than at the hA₁AR. For example, the hA_{2A}AR affinity increased substantially to a K_i value of 1.3 μM upon replacement of 3-F **12** with 3-Cl in **15**. In contrast, the same change slightly decreased hA₃AR affinity. At the hA₁AR, only 10 to 30% of binding inhibition was typically seen at 10 μM for a variety of substitutions.

The SAR was extended by the analysis of eleven analogues prepared in the N^6 -(3-chlorobenzyl) series (**27** – **36**). The effect in **27** of adding a phenyl group to the ethynyl substituent of the simpler acetylene derivative **6** was complete retention of the affinity at hA₃AR and a reduction of the hA₁AR affinity from $K_i = 174$ nM to >10 μ M, thus providing high selectivity. Furthermore, with only marginal binding of **27** at the hA_{2A}AR, the hA₃AR selectivity was roughly 10,000-fold in comparison to both hA₁AR and hA_{2A}AR. For comparison, by adding a *n*-propyl chain in **7** rather than a phenyl ring, the hA₁AR affinity was reduced only 6-fold in comparison to **6**, and the hA_{2A}AR affinity appeared to be increased. Thus, a flat aryl ring rather than a flexible alkyl chain provides the appropriate geometry for hA₃AR selectivity. A potent A₃AR ligand **34** in the N^6 -(3-chlorobenzyl) series containing a rigid, linearly extended 2-*p*-biphenylethynyl group served as a model ligand for receptor docking due to its steric and conformational constraints. It displayed a K_i value at the hA₃AR of 3.06 nM and exceptionally high selectivity in comparison to the hA₁ and hA_{2A}ARs (no inhibition observed). The hA₃AR affinities of **34** and the corresponding N^6 -methyl analogue **24** were equal. Thus, the combination of 2-arylethynyl, 5'-*N*-methyluronamide, and N^6 -3-chlorobenzyl substitution preserved the hA₃AR selectivity of (N)-methanocarba nucleosides, even for large 2-arylethynyl moieties.

Species differences in the binding affinity of the nucleoside derivatives were explored. Nanomolar A₃AR affinity was maintained in a murine species only for the N^6 -(substituted benzyl) series (Figure 1). The N^6 -methyl-2-arylethynyl derivatives **13** and **14** were determined to be ~70-fold weaker at the mA₃AR than at the hA₃AR, consistent with the previously reported reduced affinity at mA₃AR of N^6 -methyl-2-Cl derivative **8**.²¹ The mA₃AR/mA₁AR selectivity in the N^6 -methyl series was enhanced with the elongation and rigidification of the C2 substituent. However, with N^6 -3-chlorobenzyl substitution, elongation at C2 did not significantly reduce affinity at the mA₃AR compared to hA₃AR (except for a 3-fold reduction for the elongated biaryl derivative **34**). In the N^6 -3-chlorobenzyl series, particularly high selectivity compared to mA₁AR and mA_{2A}AR was generally present. There was greater variability in the degree of binding inhibition at mA₁AR than at mA_{2A}AR. Elongation of a 2-ethynyl group in **6** with a straight alkyl chain in **7** reduced mA₃AR affinity by 7-fold, but elongation with a phenyl ring in **27** only slightly reduced mA₃AR affinity. The most potent derivative at the mA₃AR was the *p*-aminophenyl analogue **32** with a K_i value of 0.82 nM. Curiously, although this derivative remained selective, its A₁AR affinity was enhanced over other members of the series at both in mouse (K_i 261 nM) and human (K_i 1520 nM).

Functional data were determined in an assay consisting of hA₃AR-induced inhibition of the production of adenosine 3',5'-cyclic phosphate (cAMP) in membranes of CHO cells expressing the hA₃AR (Table 1).³⁴ Inhibition by 10 μ M NECA (**48**, 5'-*N*-ethylcarboxamidoadenosine) was set at 100% relative efficacy. The novel (N)-methanocarba 5'-*N*-methyluronamide derivatives at 10 μ M were predominantly full agonists at the A₃AR, with a few analogues showing relative efficacy of 80% or less (*p*-fluoro **13**, *t*-butyl-phenyl **22**, and 1-pyrene **35** derivatives). A full concentration response curve in hA₃AR-mediated inhibition of adenylate cyclase for 3,4-difluoro analogue **31** provided an EC₅₀ value of 1.2 \pm 0.7 nM (Figure 2), i.e. slightly more potent than its binding affinity.

Molecular modeling

A homology model of the hA₃AR based on an agonist-bound hA_{2A}AR X-ray structure (PDB code 3QAK)²⁵ was used to study the putative interactions between the C2-substituted agonist **34** and the A₃AR. The binding mode of **34** obtained after Induced Fit docking (IFD)³⁵ revealed the following binding interactions of the ligand (Figure 3). The key residues embedding the adenosine moiety of the agonists in the receptor binding site are

mostly conserved among AR subtypes. The 3'- and 2'-hydroxyl groups were located in proximity to Ser271 (7.42) and His272 (7.43), respectively, and could form H-bonds with these residues. The NH group of the 5'-*N*-methylcarboxamido moiety was involved in H-bonding with the side chain hydroxyl group of Thr94 (3.36). Both the 6-amino group and the N7 atom of the adenine ring H-bonds with Asn250 (6.55). A π - π interaction was observed between the adenine ring of **34** and Phe168 (EL2), while the side chains of Leu246 (6.51) and Ile268 (7.39) offered CH- π interactions to the adenine moiety of **34**. The ligand-receptor interactions observed in the present model were in good agreement with the data of site-directed mutagenesis and with our previously published models of ARs, including the studies of AR agonists docked to the A_{2A}AR crystal structure.³⁶⁻³⁸ In the model obtained, the 3-chlorobenzyl ring of docked **34** was located in the hydrophobic pocket formed by Val169 (EL2), Met174 (5.35), Met172 (5.33), Ile253 (6.58), and Leu264 (7.35). More precisely, the *N*⁶-3-chlorobenzyl substituent of **34** was locked in the hydrophobic pocket of the A₃AR among TM5, TM6, TM7, and EL2 by CH- π interactions with the side chains of Val169 (EL2) and Ile253 (6.58). Ile253 (6.58) is not conserved among the ARs: in A₁, A_{2A} and A_{2B} the residue at position 6.58 is a smaller threonine. Moreover, favorable interactions between the backbone group of Met172 (5.33) and the chloro atom stabilized the compound in the binding site.

The arylethynyl substituent at the C2 position of **34** was oriented toward the extracellular part of the A₃AR in close proximity to TM2. A_{2A}AR is characterized by four constraining disulfide bridges in the extracellular domains, unlike the A₃AR, which has only one disulfide bond in that region. Thus, we expected the A₃AR to be more subject to reorganization of the TMs. The disulfide bond between Cys77 (3.25) and Cys166 (EL2) is conserved not only among the AR subtypes but also among the family A GPCRs, and it is crucial for the expression and the function of the receptors. This disulfide bond involving Cys166 holds in place the backbone of two neighboring EL2 residues that are important in ligand coordination, i.e. Gln167 and Phe168. Two other disulfide bridges of A_{2A}AR are between EL1 and EL2, namely between Cys71 and Cys159 and between Cys74 and Cys146. Another disulfide bond involves the two cysteines in EL3, Cys259 and Cys262. It has been speculated that the presence within the extracellular domains of the three disulfide bridges unique to A_{2A}AR is not crucial for the tertiary structure and the stability of the receptor, but is indeed important for ligand recognition.³⁹ From the structural point of view, from a comparison between the A_{2A}AR structure and other GPCR structures, the presence of the two disulfide bridges between EL1 and EL2 forced the extracellular terminal of TM2 toward the TM bundle, thus reducing the size of the pocket embedding the agonist C2-substituents.

The IFD procedure applied to these rigid, extended A₃AR agonists at the A_{2A}AR-based model of A₃AR was unable to accommodate the long and straight arylethynyl substituent at the C2 position due to a steric clash with the TM2 residues. In particular, the phenyl ring of the *N*⁶-methyl 2-phenylethynyl derivative **9**, a high affinity agonist at A₃AR, was clearly clashing with Ser73 in TM2, suggesting that the orientations of the extracellular terminal of TM2 and the EL1 in the A_{2A}AR-based model of A₃AR were not optimal for the accessibility of these methanocarpa derivatives to the A₃AR binding site.

New hybrid models of the A₃AR (Figure 3) were built using different templates for the homology modeling of the extracellular part of TM2, namely an agonist-bound human β_2 adrenergic receptor crystallographic structure (designated A₃AR- β_2 adr)⁴⁰ and the structure of the opsin in the activated state (designated A₃AR-ops).⁴¹ In the hybrid A₃AR model based on both the A_{2A}AR and the β_2 -adrenergic receptor structures, the extracellular extremity of TM2 moved outward by about 4 Å at the C α atom of Ser73. This movement created a larger pocket for the C2 arylethynyl substituents of the A₃AR agonists, thereby allowing derivatives such as agonist **9** to dock in the binding cavity without steric clashes

with TM2. Nevertheless, the docking of the N^6 -methyl 2-biphenylethynyl agonist **24** to the binding site of the A_3AR - β_2adr model did not produce any reasonable pose due to the steric clash between the distal phenyl ring of the compound and the residues in TM2. The unfit docked pose of **24** to the A_3AR - β_2adr model of A_3AR suggested that a larger pocket for the longer C2-substituted agonists was needed.

The outward movement of the extracellular terminal of TM2 in the hybrid A_3AR -ops model was by approximately 7 Å at the C α of Ser73, with the creation of a larger pocket for the accessibility of C2 substituents of the present rigid chain-extended A_3AR agonists, such as compounds **24** and **34**. The docking poses of **24** and **34** in the A_3AR -ops model showed the biphenylethynyl moiety of the C2 chain pointing toward the extracellular environment. The dihedral angle between the two phenyl rings was approximately 30–40°, making the C2 chain non-coplanar with the ethynyl moiety. The biphenylethynyl side chain was stabilized by favorable hydrophobic interactions with residues in TM2, EL2, and TM7, namely Ile268 (7.39), Tyr265 (7.36), Val72 (2.64), Leu264 (7.35), Phe168 (EL2), and the carbon chain of Gln167 (EL2). The side chain of Gln167, after the IFD optimization, pointed away from the binding cavity, opening the cavity to the agonists. The docking pose of **34** showed the distal phenyl ring of the C2 chain between the carbon chain of Gln167 and the aromatic ring of Tyr265. Tyr265 is in the wall of the binding pocket, but π interactions with the ligand were not evident. An analogue **22** that deviated from planarity because of the branched *t*-Bu group was significantly less potent in h A_3AR binding. The presence of a halogen atom at the *o*-, *m*- or *p*-positions of the phenyl ring in the C2 chain was studied in the binding sites of A_3AR models and the $A_{2A}AR$ crystal structure in order to understand the gain of affinity of compounds **15** and **30** at the $A_{2A}AR$. The *m*-Cl atoms of the C2 side chain of **15** and **30** in the predicted orientations in the A_3AR -ops model were located between Tyr271 and Gln167 (EL2), locked in the pocket by interactions between the halogen atom of the compounds and the OH group of Tyr271 and the side chain CO group of Gln167. The correspondent residue of Gln167 in human $A_{2A}AR$ is the hydrophobic and bulky Leu167. Nevertheless, in the docked poses of compounds **15** and **30** in the binding site of $A_{2A}AR$, the *m*-Cl atom was able to generate strong interactions with the hydroxyl groups and the aromatic moieties of Tyr271 (7.35) and Tyr9 (1.35) of $A_{2A}AR$. Instead, the orientation of the *o*-Cl atom of the docked agonists **14** and **29** was not optimal to create interactions with the side chain of Tyr271 (7.35) of $A_{2A}AR$. On the other hand, in the docked complexes of **14** and **29** with the A_3AR -ops model, the *o*-Cl atom was located between Tyr265 (7.35) and Val169 (EL2), creating favorable interactions with the OH group of Tyr265 and the backbone NH group of Val169. The residue corresponding to Val169 in the $A_{2A}AR$ is Glu169, of which the side chain was oriented such that the γ -carboxyl group interacted with the backbone NH group, i.e. no longer available to interact with the *o*-Cl atom of **14** or **29**.

Discussion

In previous studies,¹³ the SAR in AR binding was studied for two series of ribonucleosides that are particularly suited for selectivity at the h A_3AR : N^6 -methyl and N^6 -3-halobenzyl. N^6 -3-Halobenzyl substitution is greatly favored for maintaining selectivity of ribosides at the A_3AR in mouse and rat. Upon addition of the (N)-methanocarba modification,²¹ a rise in affinity was observed at the mA $_1$ AR for certain 2-chloroadenine analogues, leading to a reduction of AR selectivity in murine species. However, straight chain alkynyl groups at the C2 position, such as pentynyl **7**, alleviated this problem by reducing affinity at the mA $_1$ AR. Substitution with 2-arylethynyl groups was not examined in the (N)-methanocarba series of A_3AR agonists by Melman et al.,²¹ but we have introduced this modification in the present study.

Previously, in the ribose-5'-uronamide series, combination of 2-phenylalkynyl groups with various bulky N^6 substituents was not additive in its effect on A_3AR affinity. In a series of A_3AR -selective N^6 -aryleurea derivatives, a 2-phenylalkynyl group reduced the rA_3AR affinity in comparison to a 2-chloro analogue containing the same bulky N^6 -aryleurea, although selectivity was increased.⁴² The combination of N^6 -(substituted benzyl) groups and a 2-phenylethynyl modification produced much lower affinity in hA_3AR binding than the same structure with H at the C2 position.²⁴ A study of 2-pyrazolyl- N^6 -substituted adenosine derivatives concluded that bulky substitutions at those two positions generally did not benefit from additivity in hA_3AR binding affinity.^{13c}

We have now explored the effects of various 2-(arylethynyl) groups at the adenine C2 position on AR affinity of (N)-methanocarpa 5'- N -methyluronamido nucleosides. The resulting analogues (both N^6 -methyl and N^6 -3-halobenzyl) were full agonists of the hA_3AR of nanomolar affinity that were consistently highly selective (typically >1000-fold vs. hA_1AR and $hA_{2A}AR$). The most potent and selective N^6 -methyl compounds were *p*-F **13** and *o*-Cl **14** analogues. At the mA_3AR , selectivity generally remained, but for N^6 -methyl derivatives the high affinities achievable were somewhat lower than at hA_3AR . Thus, the combination of a 2-(arylethynyl) group and large N^6 substitutions was better tolerated at the A_3AR in the methanocarpa series than in the 9-ribose series, as characterized in earlier reports. There is also a broad flexibility of substitution of the 2-(arylethynyl) moiety, with halo, hydrophobic, and hydrophilic substitutions without losing A_3AR selectivity. This feature could also benefit specific pharmacological characteristics, such as pharmacokinetic properties. The 3,4-difluoro substitution of **31** might impede possible *in vivo* metabolic transformation of this ring (cf. P2Y₁₂ receptor antagonist Ticagrelor^{1b}).

The pharmacokinetic properties of these analogues have not been measured. However, they represent an increase in hydrophobicity, as well as selectivity, in comparison to most widely used A_3AR agonists. For example, the cLog P values of potent 2-chlorophenylethynyl **29**, 4-fluorophenylethynyl **30** and 3,4-fluorophenylethynyl **31** derivatives are 4.65, 4.08 and 4.15, respectively. The cLog P values of more polar ribosides **1** and **2** are 0.48 and 1.20, respectively, which is possibly less desirable for full bioavailability. The total polar surface area of **29** is 121.9 Å², which is a more favorable value for one of the physical parameters that predicts drug-likeness compared to 131.1 Å² for both **1** and **2**.⁴³

Even large, planar polyaromatic groups at C2 (separated by an acetylene moiety) were tolerated and retained nanomolar affinity. In binding to the $A_{2A}AR$, a 2-(2-(naphth-1-yl)ethoxy) analogue bound with high affinity, and the location of the naphthyl group was predicted by docking.⁴⁴ In the present study, the size of the polycyclic C2 groups, i.e. in the potent phenanthrene-ethynyl derivative **26**, exceeded that of all previous AR ligands. The 1-pyrene derivative **35** and its less potent 4-pyrene isomer **36** represent different sites of attachment of the 2-ethynyl moiety to the same large polyaromatic group. In receptor binding experiments, differences were observed that could provide insight into the geometry of the binding site considering the spatial and conformational constraints of these agonists. The 4-pyrene derivative **36** (with one additional ring added) has a close analogue in the N^6 -methyl series, i.e. **26**.

These observations were subjected to molecular modeling analysis, which also predicted useful analogues to be synthesized. The ribose moiety is tightly anchored through a H-bond network involving TM3 and TM7, and the geometry of the unnatural glycosidic bond to the nucleobase is restricted. Thus, there is little angular flexibility of the extended, rigid C2 substituents. Thus, anchoring of the adenosine moiety to conserved amino acid residues provides a framework for exploring the region surrounding the linearly extended C2 substituent. The placement of a 2-arylethynyl substituent in the hA_3AR binding site was

predicted by Dal Ben et al. using the inactive structure of the hA_{2A}AR as template, and the orientation is similar to that found here.^{23b} However, the present study predicts the docking mode with greater detail and confidence, because the homology model is based on the agonist-bound A_{2A}AR structure.²⁵ With the present set of rigidified analogues, we have located a very large hydrophobic pocket on the receptor that depends on an outward displacement of TM2 in order to accommodate multiple fused rings. Thus, the binding would be allowed by the plasticity of the receptor structure to attain a ligand-specific reorganization. The reduction of hA₃AR affinity for the larger C2 substituents in **35** and **36** suggests that although TM2 could shift position to accommodate such groups, there is an energetic cost for these more bulky planar polyaromatic groups. As the movement of TM2 increases, some stabilizing interactions with other regions of the receptor would be progressively lost.

The A₃AR homology model built based exclusively on the crystal structure of an agonist-bound A_{2A}AR required an adjustment of the position of TM2, which was based on the orientation of TM2 in other agonist-bound or activated GPCR templates, i.e. the β₂-adrenergic receptor or opsin. The most successful template for TM2 was the structure of opsin, which displaced the upper part of TM2 relative to the agonist-bound A_{2A}AR by ~7 Å. Thus, we predict an outward displacement of TM2 similar to the opsin structure, which is specific for agonists containing rigid C2 extensions. The inability of the A_{2A}AR to rearrangement might contribute to the A₃AR selectivity of these compounds.

The displacement of one or more TMs to accommodate a sterically bulky ligand, assuming that there are no other constraints on the helix such as a proximal disulfide bond, might be a general phenomenon in GPCRs. The ability of the helices to readjust position or “breathe” to enable a larger ligand to bind has already been proposed, specifically with respect to “multi-conformational space of the antagonist-like state of the human A₃ receptor”.⁴⁵ The example of altered A_{2A}AR conformation specific to binding of a sterically extended agonist 6-(2,2-diphenylethylamino)-9-((2*R*,3*R*,4*S*,5*S*)-5-(ethylcarbamoyl)-3,4-dihydroxytetrahydrofuran-2-yl)-*N*-(2-(3-(1-(pyridin-2-yl)piperidin-4-yl)ureido)ethyl)-9H-purine-2-carboxamide (**59**, UK-432097) was already documented in the X-ray structure.²⁵ In particular, outward movements of EL3 and extracellular portion of TM7 were associated exclusively with this bulky, multifunctionalized agonist.

The implications for receptor coupling and signaling of this type of displacement, such as the agonist-dependent movement of TM2 that we predict here, are unknown. If this conformational change associated with a family of ligands is propagated to the intracellular regions, we speculate that there could differential effects on multiple signaling pathways, and might eventually provide a rational basis for the design of biased GPCR agonists.

The enhancement of A_{2A}AR affinity in the 2-(3-chlorophenylethynyl) analogues **15** and **30** indicated a consistent interaction with a specific site on the hA_{2A}AR. Modeling analysis suggested halogen-π interactions⁴⁶ with two tyrosine residues in the C2 binding cavity of A_{2A}AR, namely Tyr271 (7.36) and Tyr9 (1.35), to explain the activity of the 2-(3-chlorophenylethynyl) methanocarpa adenosine derivatives **15** and **30** at the A_{2A}AR.

The freedom to insert polyaromatic ring systems on the 2-ethynyl group suggests inclusion of reporter groups, such as fluorescent dye moieties at this site. In fact, the pyrene analogue **35** is highly fluorescent and could be explored as spectroscopic probes of moderate affinity for receptor binding experiments. The fluorescent properties of pyrene are sensitive to the environment. The *p*-amino derivative **32** has a high affinity at both the mA₃AR and hA₃AR, and could potentially be derivatized for radioisotope incorporation or affinity cross-linking. We are also interested in the design of radiofluorinated nucleosides for positron emission

tomographic (PET) imaging of the A₃AR *in vivo*.⁴⁷ Several fluorinated species in this study could provide the basis for incorporation of ¹⁸F into a high affinity A₃AR agonist.

In conclusion, we have found a new series of highly potent and selective series of A₃AR agonists containing combined substitution of the (N)-methanocarpa ring system and arylethynyl groups at the adenine C2 position. The binding affinities demonstrated high tolerance of steric bulk and ring substitution by extension at the C2 position, with many aryl groups providing K_i values in the nM range. Molecular modeling suggests that this reflects conformational plasticity of the A₃AR. Potent agonist ligands should be useful in future pharmacological studies of the antiinflammatory, anticancer and antiischemic properties of A₃AR agonists.

Experimental Section

Chemical synthesis

Materials and instrumentation—L-ribose, and other reagents and solvents were purchased from Sigma-Aldrich (St. Louis, MO). Alcohol derivative **39** was prepared as reported.²⁸ ¹H NMR spectra were obtained with a Bruker 400 spectrometer using CDCl₃ and CD₃OD as solvents. Chemical shifts are expressed in δ values (ppm) with tetramethylsilane (δ 0.00) for CDCl₃ and water (δ 3.30) for CD₃OD. TLC analysis was carried out on glass sheets precoated with silica gel F₂₅₄ (0.2 mm) from Aldrich. The purity of final nucleoside derivatives was checked using a Hewlett–Packard 1100 HPLC equipped with a Zorbax SB-Aq 5 μm analytical column (50 × 4.6 mm; Agilent Technologies Inc, Palo Alto, CA). Mobile phase: linear gradient solvent system: 5 mM TBAP (tetrabutylammonium dihydrogenphosphate)-CH₃CN from 80:20 to 0:100 in 13 min; the flow rate was 0.5 mL/min. Peaks were detected by UV absorption with a diode array detector at 230, 254, and 280 nm. All derivatives tested for biological activity showed >95% purity by HPLC analysis (detection at 254 nm). Low-resolution mass spectrometry was performed with a JEOL SX102 spectrometer with 6-kV Xe atoms following desorption from a glycerol matrix or on an Agilent LC/MS 1100 MSD, with a Waters (Milford, MA) Atlantis C18 column. High resolution mass spectroscopic (HRMS) measurements were performed on a proteomics optimized Q-TOF-2 (Micromass-Waters) using external calibration with polyalanine, unless noted. Observed mass accuracies are those expected based on known performance of the instrument as well as trends in masses of standard compounds observed at intervals during the series of measurements. Reported masses are observed masses uncorrected for this time-dependent drift in mass accuracy. Synthetic procedures for **45** – **47** are in Supporting information. LogP and total polar surface area values were calculated using ChemBioDraw Ultra (Version 12.0.3, PerkinElmer, Boston, MA).

(1S,2R,3S,4R,5S)-2,3-Dihydroxy-N-methyl-4-(6-(methylamino)-2-(phenylethynyl)-9H-purin-9-yl)bicyclo[3.1.0]hexane-1-carboxamide (9)—A

solution of compound **45a** (29 mg, 0.06 mmol) in methanol (2 mL) and 10% trifluoromethane sulfonic acid (2 mL) was heated at 70 °C for 5 h. Solvent was evaporated under vacuum, and the residue was purified on flash silica gel column chromatography (CH₂Cl₂:MeOH = 25:1) to give compound **9** (21 mg, 81%) as a syrup. ¹H NMR (CD₃OD) δ 8.12 (s, 1H), 7.67-7.65 (m, 2H), 7.47-7.43 (m, 2H), 5.06 (d, *J* = 5.2 Hz, 1H), 4.08 (d, *J* = 6.4 Hz, 1H), 3.15 (br s, 3H), 2.84 (s, 3H), 2.13-2.10 (m, 1H), 1.88 (t, *J* = 5.2 Hz, 1H), 1.41-1.39 (m, 1H). HRMS calculated for C₂₂H₂₃N₆O₃ (M + H)⁺: 419.1832; found 419.1818.

(1S,2R,3S,4R,5S)-2,3-Dihydroxy-N-methyl-4-(6-(methylamino)-2-(pyridin-2-ylethynyl)-9H-purin-9-yl)bicyclo[3.1.0]hexane-1-carboxamide (10)—Compound **10** (80%) was prepared from compound **46** following the same method as used for

compound **9**. ^1H NMR (CD_3OD) δ 8.65 (s, 1H), 8.01 (s, 1H), 7.91–7.97 (m, 1H), 7.87 (d, J = 8.8 Hz, 1H), 7.53–7.48 (m, 1H), 5.15 (d, J = 5.6 Hz, 1H), 4.09 (d, J = 8.4 Hz, 1H), 3.14 (br s, 3H), 2.83 (s, 3H), 2.13–2.06 (m, 1H), 1.85 (t, J = 5.2 Hz, 1H), 1.42–1.40 (m, 1H). HRMS calculated for $\text{C}_{21}\text{H}_{22}\text{N}_7\text{O}_3$ ($\text{M} + \text{H}$) $^+$: 420.1784; found 420.1797.

(1S,2R,3S,4R,5S)-4-(2-((2-Fluorophenyl)ethynyl)-6-(methylamino)-9H-purin-9-yl)-2,3-dihydroxy-N-methylbicyclo[3.1.0]hexane-1-carboxamide (11)—

Compound **11** (82%) was prepared from compound **45b** following the same method as used for compound **9**. ^1H NMR (CD_3OD) δ 8.11 (s, 1H), 7.49–7.39 (m, 3H), 7.25–7.20 (m, 1H), 5.06 (d, J = 5.2 Hz, 1H), 4.9 (s, 1H), 4.02 (d, J = 6.8 Hz, 1H), 3.15 (br s, 1H), 2.84 (s, 3H), 2.13–2.10 (m, 1H), 1.88 (t, J = 4.8 Hz, 1H), 1.41–1.38 (m, 1H). HRMS calculated for $\text{C}_{22}\text{H}_{22}\text{FN}_6\text{O}_3$ ($\text{M} + \text{H}$) $^+$: 437.1737; found 437.1753.

(1S,2R,3S,4R,5S)-4-(2-((3-Fluorophenyl)ethynyl)-6-(methylamino)-9H-purin-9-yl)-2,3-dihydroxy-N-methylbicyclo[3.1.0]hexane-1-carboxamide (12)—

Compound **12** (78%) was prepared from compound **45c** following the same method as used for compound **9**. ^1H NMR (CD_3OD) δ 8.11 (s, 1H), 7.67 (t, J = 6.0 Hz, 1H), 7.52–7.47 (m, 1H), 7.28–7.22 (m, 2H), 5.07 (d, J = 6.8 Hz, 1H), 4.03 (d, J = 6.8 Hz, 1H), 3.13 (br s, 1H), 2.84 (s, 3H), 2.13–2.10 (m, 1H), 1.88 (t, J = 4.8 Hz, 1H), 1.41–1.40 (m, 1H). HRMS calculated for $\text{C}_{22}\text{H}_{22}\text{FN}_6\text{O}_3$ ($\text{M} + \text{H}$) $^+$: 437.1737; found 437.1718.

(1S,2R,3S,4R,5S)-4-(2-((4-Fluorophenyl)ethynyl)-6-(methylamino)-9H-purin-9-yl)-2,3-dihydroxy-N-methylbicyclo[3.1.0]hexane-1-carboxamide (13)—

Compound **13** (81%) was prepared from compound **45d** following the same method as used for compound **9**. ^1H NMR (CD_3OD) δ 8.11 (s, 1H), 7.75–7.68 (m, 2H), 7.23–7.18 (m, 2H), 5.05 (d, J = 6.0 Hz, 1H), 4.02 (d, J = 6.4 Hz, 1H), 3.14 (br s, 3H), 2.84 (s, 3H), 2.13–2.10 (m, 1H), 1.89 (t, J = 4.8 Hz, 1H), 1.41–1.39 (m, 1H). HRMS calculated for $\text{C}_{22}\text{H}_{22}\text{FN}_6\text{O}_3$ ($\text{M} + \text{H}$) $^+$: 437.1737; found 437.1722.

(1S,2R,3S,4R,5S)-4-(2-((2-Chlorophenyl)ethynyl)-6-(methylamino)-9H-purin-9-yl)-2,3-dihydroxy-N-methylbicyclo[3.1.0]hexane-1-carboxamide (14)—

Compound **14** (85%) was prepared from compound **45e** following the same method as used for compound **9**. ^1H NMR (CD_3OD) δ 8.11 (s, 1H), 7.72 (d, J = 7.2 Hz, 1H), 7.54 (d, J = 7.2 Hz, 1H), 7.46–7.36 (m, 2H), 5.10 (d, J = 6.4 Hz, 1H), 4.04 (d, J = 6.8 Hz, 1H), 3.15 (br s, 3H), 2.83 (s, 3H), 2.12–2.08 (m, 1H), 1.86 (t, J = 4.8 Hz, 1H), 1.41–1.39 (m, 1H). HRMS calculated for $\text{C}_{22}\text{H}_{22}\text{ClN}_6\text{O}_3$ ($\text{M} + \text{H}$) $^+$: 453.1442; found 453.1449.

(1S,2R,3S,4R,5S)-4-(2-((3-Chlorophenyl)ethynyl)-6-(methylamino)-9H-purin-9-yl)-2,3-dihydroxy-N-methylbicyclo[3.1.0]hexane-1-carboxamide (15)—

Compound **15** (82%) was prepared from compound **45f** following the same method as used for compound **9**. ^1H NMR (CD_3OD) δ 8.11 (s, 1H), 7.67 (s, 1H), 7.59 (d, J = 7.2 Hz, 1H), 7.49–7.42 (m, 2H), 5.06 (d, J = 6.4 Hz, 1H), 4.02 (d, J = 6.8 Hz, 1H), 3.14 (br s, 3H), 2.84 (s, 3H), 2.13–2.10 (m, 1H), 1.88 (t, J = 4.8 Hz, 1H), 1.41–1.39 (m, 1H). HRMS calculated for $\text{C}_{22}\text{H}_{22}\text{ClN}_6\text{O}_3$ ($\text{M} + \text{H}$) $^+$: 453.1442; found 453.1442.

(1S,2R,3S,4R,5S)-4-(2-((4-Chlorophenyl)ethynyl)-6-(methylamino)-9H-purin-9-yl)-2,3-dihydroxy-N-methylbicyclo[3.1.0]hexane-1-carboxamide (16)—

Compound **16** (84%) was prepared from compound **45g** following the same method as used for compound **9**. ^1H NMR (CD_3OD) δ 8.10 (s, 1H), 7.64 (d, J = 8.4 Hz, 2H), 7.46 (d, J = 8.4 Hz, 2H), 5.06 (d, J = 5.6 Hz, 1H), 4.88 (s, 1H), 4.02 (d, J = 6.4 Hz, 1H), 3.15 (br s, 3H), 2.84 (s, 3H), 2.13–2.09 (m, 1H), 1.88 (t, J = 4.8 Hz, 1H), 1.41–1.38 (m, 1H). HRMS calculated for $\text{C}_{22}\text{H}_{22}\text{ClN}_6\text{O}_3$ ($\text{M} + \text{H}$) $^+$: 453.1460; found 453.1454.

(1*S*,2*R*,3*S*,4*R*,5*S*)-4-(2-((4-Bromophenyl)ethynyl)-6-(methylamino)-9*H*-purin-9-yl)-2,3-dihydroxy-*N*-methylbicyclo[3.1.0]hexane-1-carboxamide (17)—

Compound **17** (76%) was prepared from compound **45h** following the same method as used for compound **9**. ¹H NMR (CD₃OD) δ 8.10 (s, 1H), 7.62 (d, *J* = 8.8 Hz, 2H), 7.56 (d, *J* = 8.4 Hz, 2H), 5.05 (d, *J* = 6.8 Hz, 1H), 4.88 (s, 1H), 4.02 (d, *J* = 6.4 Hz, 1H), 3.14 (br s, 3H), 2.84 (s, 3H), 2.13-2.09 (m, 1H), 1.88 (t, *J* = 5.2 Hz, 1H), 1.41-1.38 (m, 1H). HRMS calculated for C₂₂H₂₂BrN₆O₃ (M + H)⁺: 497.0937; found 497.0948.

(1*S*,2*R*,3*S*,4*R*,5*S*)-4-(2-((3-Aminophenyl)ethynyl)-6-(methylamino)-9*H*-purin-9-yl)-2,3-dihydroxy-*N*-methylbicyclo[3.1.0]hexane-1-carboxamide (18)—

Compound **18** (67%) was prepared from compound **45i** following the same method as used for compound **9**. ¹H NMR (CD₃OD) δ 8.09 (s, 1H), 7.14 (t, *J* = 8.0 Hz, 1H), 6.98-6.94 (m, 2H), 6.80-6.78 (m, 1H), 5.06 (d, *J* = 5.6 Hz, 1H), 4.02 (d, *J* = 6.4 Hz, 1H), 3.15 (br s, 3H), 2.85 (s, 3H), 2.12-2.09 (m, 1H), 1.87 (t, *J* = 4.8 Hz, 1H), 1.41-1.39 (m, 1H). HRMS calculated for C₂₂H₂₂N₇O₃ (M + H)⁺: 432.1784; found 432.1799.

(1*S*,2*R*,3*S*,4*R*,5*S*)-4-(2-((3,4-Difluorophenyl)ethynyl)-6-(methylamino)-9*H*-purin-9-yl)-2,3-dihydroxy-*N*-methylbicyclo[3.1.0]hexane-1-carboxamide (19)—

Compound **19** (83%) was prepared from compound **45j** following the same method as used for compound **9**. ¹H NMR (CD₃OD) δ 8.12 (s, 1H), 7.58-7.50 (m, 1H), 7.50-7.48 (m, 1H), 7.40-7.34 (m, 1H), 5.06 (d, *J* = 6.4 Hz, 1H), 4.02 (d, *J* = 6.4 Hz, 1H), 3.14 (br s, 3H), 2.84 (s, 3H), 2.13-2.09 (m, 1H), 1.88 (t, *J* = 4.8 Hz, 1H), 1.41-1.40 (m, 1H). HRMS calculated for C₂₂H₂₁F₂N₆O₃ (M + H)⁺: 455.1643; found 455.1639.

(1*S*,2*R*,3*S*,4*R*,5*S*)-4-(2-((3,5-Difluorophenyl)ethynyl)-6-(methylamino)-9*H*-purin-9-yl)-2,3-dihydroxy-*N*-methylbicyclo[3.1.0]hexane-1-carboxamide (20)—

Compound **20** (84%) was prepared from compound **45k** following the same method as used for compound **9**. ¹H NMR (CD₃OD) δ 8.12 (s, 1H), 7.31-7.26 (s, 2H), 7.14-7.09 (m, 1H), 7.49-7.42 (m, 2H), 5.06 (d, *J* = 5.2 Hz, 1H), 4.89 (s, 1H), 4.03 (d, *J* = 6.4 Hz, 1H), 3.14 (br s, 3H), 2.84 (s, 3H), 2.12-2.09 (m, 1H), 1.88 (t, *J* = 4.8 Hz, 1H), 1.41-1.39 (m, 1H). HRMS calculated for C₂₂H₂₁F₂N₆O₃ (M + H)⁺: 455.1643; found 455.1630.

(1*S*,2*R*,3*S*,4*R*,5*S*)-4-(2-((4-Ethylphenyl)ethynyl)-6-(methylamino)-9*H*-purin-9-yl)-2,3-dihydroxy-*N*-methylbicyclo[3.1.0]hexane-1-carboxamide (21)—

Compound **21** (79%) was prepared from compound **45l** following the same method as used for compound **9**. ¹H NMR (CD₃OD) δ 8.09 (s, 1H), 7.57 (d, *J* = 8.0 Hz, 2H), 7.29 (d, *J* = 8.0 Hz, 2H), 5.06 (d, *J* = 5.2 Hz, 1H), 4.91 (s, 1H), 4.02 (d, *J* = 6.4 Hz, 1H), 3.15 (br s, 3H), 2.84 (s, 3H), 2.74-2.68 (m, 2H), 2.13-2.09 (m, 1H), 1.88 (t, *J* = 4.8 Hz, 1H), 1.41-1.38 (m, 1H), 1.30 (t, *J* = 7.6 Hz, 3H). HRMS calculated for C₂₄H₂₇N₆O₃ (M + H)⁺: 447.2145; found 447.2130.

(1*S*,2*R*,3*S*,4*R*,5*S*)-4-(2-((4-*tert*-Butylphenyl)ethynyl)-6-(methylamino)-9*H*-purin-9-yl)-2,3-dihydroxy-*N*-methylbicyclo[3.1.0]hexane-1-carboxamide (22)—

Compound **22** (83%) was prepared from compound **45m** following the same method as used for compound **9**. ¹H NMR (CD₃OD) δ 8.10 (s, 1H), 7.59 (d, *J* = 8.4 Hz, 2H), 7.50 (d, *J* = 8.4 Hz, 2H), 5.06 (d, *J* = 6.4 Hz, 1H), 4.02 (d, *J* = 6.4 Hz, 1H), 3.15 (br s, 3H), 2.85 (s, 3H), 2.13-2.10 (m, 1H), 1.88 (t, *J* = 4.8 Hz, 1H), 1.41-1.39 (m, 10H). HRMS calculated for C₂₆H₃₁N₆O₃ (M + H)⁺: 475.2458; found 475.2450.

(1*S*,2*R*,3*S*,4*R*,5*S*)-4-(2-((4-Acetylphenyl)ethynyl)-6-(methylamino)-9*H*-purin-9-yl)-2,3-dihydroxy-*N*-methylbicyclo[3.1.0]hexane-1-carboxamide (23)—

Compound **23** (80%) was prepared from compound **45n** following the same method as used

for compound **9**. $^1\text{H NMR}$ (CD_3OD) δ 8.11 (s, 1H), 8.06 (d, $J = 8.4$ Hz, 2H), 7.77 (d, $J = 8.0$ Hz, 2H), 5.06 (d, $J = 6.4$ Hz, 1H), 4.03 (d, $J = 6.4$ Hz, 1H), 3.15 (br s, 3H), 2.84 (s, 3H), 2.64 (s, 3H), 2.14-2.10 (m, 1H), 1.88 (t, $J = 4.8$ Hz, 1H), 1.41-1.39 (m, 1H). HRMS calculated for $\text{C}_{24}\text{H}_{25}\text{N}_6\text{O}_4$ ($\text{M} + \text{H}$) $^+$: 461.1937; found 461.1937.

(1S,2R,3S,4R,5S)-4-(2-(Biphenyl-4-ylethynyl)-6-(methylamino)-9H-purin-9-yl)-2,3-dihydroxy-N-methylbicyclo[3.1.0]hexane-1-carboxamide (24)—

Compound **24** (74%) was prepared from compound **45o** following the same method as used for compound **9**. $^1\text{H NMR}$ (CD_3OD) δ 8.11 (s, 1H), 7.75-7.67 (m, 6H), 7.47 (t, $J = 7.6$ Hz, 2H), 7.38 (t, $J = 7.2$ Hz, 1H), 5.06 (d, $J = 6.0$ Hz, 1H), 4.89 (s, 1H), 4.03 (d, $J = 6.4$ Hz, 1H), 3.16 (br s, 3H), 2.84 (s, 3H), 2.13-2.10 (m, 1H), 1.89 (t, $J = 4.8$ Hz, 1H), 1.42-1.39 (m, 1H). HRMS calculated for $\text{C}_{28}\text{H}_{27}\text{N}_6\text{O}_3$ ($\text{M} + \text{H}$) $^+$: 495.2145; found 495.2141.

(1S,2R,3S,4R,5S)-2,3-Dihydroxy-N-methyl-4-(6-(methylamino)-2-(naphthalen-1-ylethynyl)-9H-purin-9-yl)bicyclo[3.1.0]hexane-1-carboxamide (25)—Compound **25** (73%) was prepared from compound **45p** following the same method as used for compound **9**. $^1\text{H NMR}$ (CD_3OD) δ 8.56 (d, $J = 7.6$ Hz, 1H), 8.11 (s, 1H), 8.00-7.90 (m, 3H), 7.68 (t, $J = 5.6$ Hz, 1H), 7.62-7.53 (m, 2H), 5.10 (d, $J = 5.2$ Hz, 1H), 4.93 (s, 1H), 4.06 (d, $J = 6.4$ Hz, 1H), 3.19 (br s, 3H), 2.79 (s, 3H), 2.15-2.12 (m, 1H), 1.89 (t, $J = 4.8$ Hz, 1H), 1.41-1.38 (m, 1H). HRMS calculated for $\text{C}_{26}\text{H}_{25}\text{N}_6\text{O}_3$ ($\text{M} + \text{H}$) $^+$: 469.1988; found 469.2005.

(1S,2R,3S,4R,5S)-2,3-Dihydroxy-N-methyl-4-(6-(methylamino)-2-(phenanthren-9-ylethynyl)-9H-purin-9-yl)bicyclo[3.1.0]hexane-1-carboxamide (26)—

Compound **26** (65%) was prepared from compound **45q** following the same method as used for compound **9**. $^1\text{H NMR}$ (CD_3OD) δ 8.84-8.77 (m, 2H), 8.66-8.63 (m, 1H), 8.26 (s, 1H), 8.12 (s, 1H), 7.97 (d, $J = 7.6$ Hz, 1H), 7.80-7.73 (m, 3H), 7.66 (t, $J = 7.2$ Hz, 1H), 5.10 (d, $J = 6.0$ Hz, 1H), 4.92 (s, 1H), 4.07 (d, $J = 6.4$ Hz, 1H), 3.20 (br s, 3H), 2.81 (s, 3H), 2.15-2.12 (m, 1H), 1.90 (t, $J = 4.8$ Hz, 1H), 1.42-1.38 (m, 1H). HRMS calculated for $\text{C}_{30}\text{H}_{27}\text{N}_6\text{O}_3$ ($\text{M} + \text{H}$) $^+$: 519.2145; found 519.2137.

(1S,2R,3S,4R,5S)-4-(6-(3-Chlorobenzylamino)-2-(phenylethynyl)-9H-purin-9-yl)-2,3-dihydroxy-N-methylbicyclo[3.1.0]hexane-1-carboxamide (27)—

$\text{PdCl}_2(\text{PPh}_3)_2$ (6.13 mg, 0.008 mmol), CuI (1.2 mg, 0.004 mmol), phenylacetylene (30 μL , 0.26 mmol) and triethylamine (60 μL , 0.4 mmol) was added to a solution of compound **44** (26 mg, 0.04 mmol) in anhydrous DMF (1 mL), and stirred at room temperature overnight. Solvent was evaporated under vacuum, and the residue was roughly purified on flash silica gel column chromatography. The resulting compound was dissolved in methanol (2 mL) and 10% trifluoromethane sulfonic acid (2 mL) and heated at 70 $^\circ\text{C}$ for 5 h. Solvent was evaporated under vacuum, and the residue was purified on flash silica gel column chromatography ($\text{CH}_2\text{Cl}_2:\text{MeOH} = 25:1$) to give compound **27** (17 mg, 76%) as a syrup. $^1\text{H NMR}$ (CD_3OD) δ 8.13 (s, 1H), 7.66-7.63 (m, 2H), 7.46-7.42 (m, 4H), 7.37-7.26 (m, 3H), 5.06 (d, $J = 5.6$ Hz, 1H), 4.9 (br s, 2H), 4.04 (d, $J = 6.4$ Hz, 1H), 2.84 (s, 3H), 2.14-2.11 (m, 1H), 1.88 (t, $J = 4.8$ Hz, 1H), 1.41-1.37 (m, 1H). HRMS calculated for $\text{C}_{28}\text{H}_{26}\text{ClN}_6\text{O}_3$ ($\text{M} + \text{H}$) $^+$: 529.1755; found 529.1740.

(1S,2R,3S,4R,5S)-4-(6-(3-Chlorobenzylamino)-2-((4-fluorophenyl)ethynyl)-9H-purin-9-yl)-2,3-dihydroxy-N-methylbicyclo[3.1.0]hexane-1-carboxamide (28)—

Compound **28** (68%) was prepared from compound **44** following the same method as used for compound **27**. $^1\text{H NMR}$ (CD_3OD) δ 8.13 (s, 1H), 7.70-7.63 (m, 2H), 7.59-7.55 (m, 1H), 7.45 (s, 1H), 7.37-7.21 (m, 3H), 7.19-7.16 (m, 1H), 5.06 (d, $J = 5.6$ Hz, 1H), 4.9 (s, 1H), 4.58 (br s, 2H), 4.04 (d, $J = 7.6$ Hz, 1H), 2.84 (s, 3H), 2.17-2.10 (m, 1H), 1.88 (t, $J = 4.8$ Hz,

1H), 1.41-1.38 (m, 1H). HRMS calculated for C₂₈H₂₅ClFN₆O₃ (M + H)⁺: 547.1661; found 547.1652.

(1S,2R,3S,4R,5S)-4-(6-(3-Chlorobenzylamino)-2-((2-chlorophenyl)ethynyl)-9H-purin-9-yl)-2,3-dihydroxy-N-methylbicyclo[3.1.0]hexane-1-carboxamide (29)—

Compound **29** (65%) was prepared from compound **44** following the same method as used for compound **27**. ¹H NMR (CD₃OD) δ 8.14 (s, 1H), 7.72-7.70 (m, 1H), 7.53 (d, *J* = 8.0 Hz, 1H), 7.47-7.25 (m, 6H), 5.11 (d, *J* = 6.8 Hz, 1H), 4.90 (s, 1H), 4.05 (d, *J* = 6.8 Hz, 1H), 2.82 (s, 3H), 2.12-2.09 (m, 1H), 1.86 (t, *J* = 4.8 Hz, 1H), 1.40-1.38 (m, 1H). HRMS calculated for C₂₈H₂₄Cl₂N₆O₃Na (M + Na)⁺: 585.1185; found 585.1167.

(1S,2R,3S,4R,5S)-4-(6-(3-Chlorobenzylamino)-2-((3-chlorophenyl)ethynyl)-9H-purin-9-yl)-2,3-dihydroxy-N-methylbicyclo[3.1.0]hexane-1-carboxamide (30)—

Compound **30** (66%) was prepared from compound **44** following the same method as used for compound **27**. ¹H NMR (CD₃OD) δ 8.15 (s, 1H), 7.66-7.57 (m, 2H), 7.48-7.26 (m, 6H), 5.07 (d, *J* = 6.4 Hz, 1H), 4.85 (s, 1H), 4.04 (d, *J* = 6.8 Hz, 1H), 2.84 (s, 3H), 2.14-2.10 (m, 1H), 1.88 (t, *J* = 4.8 Hz, 1H), 1.41-1.39 (m, 1H). HRMS calculated for C₂₈H₂₅Cl₂N₆O₃ (M + H)⁺: 563.1365; found 563.1359.

(1S,2R,3S,4R,5S)-4-(6-(3-Chlorobenzylamino)-2-((3,4-difluorophenyl)ethynyl)-9H-purin-9-yl)-2,3-dihydroxy-N-methylbicyclo[3.1.0]hexane-1-carboxamide (31)—

Compound **31** (63%) was prepared from compound **44** following the same method as used for compound **27**. ¹H NMR (CD₃OD) δ 8.14 (s, 1H), 7.58 (t, *J* = 8.8 Hz, 1H), 7.47-7.44 (m, 2H), 7.39-7.25 (m, 4H), 5.06 (d, *J* = 6.4 Hz, 1H), 4.89 (s, 1H), 4.04 (d, *J* = 6.4 Hz, 1H), 2.84 (s, 3H), 2.13-2.10 (m, 1H), 1.88 (t, *J* = 4.8 Hz, 1H), 1.41-1.38 (m, 1H). HRMS calculated for C₂₈H₂₄F₂ClN₆O₃ (M + H)⁺: 565.1566; found 565.1559.

(1S,2R,3S,4R,5S)-4-(2-((4-Aminophenyl)ethynyl)-6-(3-chlorobenzylamino)-9H-purin-9-yl)-2,3-dihydroxy-N-methylbicyclo[3.1.0]hexane-1-carboxamide (32)—

Compound **32** (59%) was prepared from compound **44** following the same method as used for compound **27**. ¹H NMR (CD₃OD) δ 8.02 (s, 1H), 7.84 (d, *J* = 8.8 Hz, 2H), 7.33-7.23 (m, 4H), 6.60 (d, *J* = 8.4 Hz, 2H), 5.17 (d, *J* = 6.4 Hz, 1H), 4.85 (s, 1H), 4.73 (br s, 2H), 4.02 (d, *J* = 6.8 Hz, 1H), 2.83 (s, 3H), 2.08-2.05 (m, 1H), 1.81 (t, *J* = 4.8 Hz, 1H), 1.41-1.37 (m, 1H). HRMS calculated for C₂₈H₂₇ClN₇O₃ (M + H)⁺: 545.1041; found 545.1045.

3-((6-(3-Chlorobenzylamino)-9-((1S,2R,3S,4R,5S)-3,4-dihydroxy-5-(methylcarbamoyl)bicyclo[3.1.0]hexan-2-yl)-9H-purin-2-yl)ethynyl)benzoic acid (33)—

PdCl₂(PPh₃)₂ (3.0 mg, 0.004 mmol), CuI (1.0 mg, 0.004 mmol), phenylacetylene (18.7 mg, 0.12 mmol) and triethylamine (20 μL, 0.2 mmol) was added to a solution of compound **44** (12.68 mg, 0.02 mmol) in anhydrous DMF (1 mL), and stirred at room temperature overnight. Solvent was evaporated under vacuum, and the residue was roughly purified on flash silica gel column chromatography. The resulting compound was dissolved in dioxane (2 mL) and 1N HCl (1.5 mL) and heated at 60 °C for 2 h. After completion of starting material, solvent was evaporated under vacuum, and the residue was purified on flash silica gel column chromatography (CH₂Cl₂:MeOH:TFA = 25:1:0.1) to give compound **33** (7 mg, 61%) as a syrup. ¹H NMR (CD₃OD) δ 8.28 (s, 1H), 8.18-8.16 (m, 1H), 8.11-8.07 (m, 1H), 7.87 (d, *J* = 7.6 Hz, 1H), 7.59-7.54 (m, 2H), 7.47 (s, 1H), 7.41-7.26 (m, 2H), 5.09 (d, *J* = 6.4 Hz, 1H), 4.91 (s, 1H), 4.05 (d, *J* = 6.4 Hz, 1H), 2.85 (s, 3H), 2.14-2.11 (m, 1H), 1.88 (t, *J* = 4.8 Hz, 1H), 1.42-1.38 (m, 1H). HRMS calculated for C₂₉H₂₆ClN₆O₅ (M + H)⁺: 573.1653; found 573.1646.

(1*S*,2*R*,3*S*,4*R*,5*S*)-4-(2-(Biphenyl-4-ylethynyl)-6-(3-chlorobenzylamino)-9*H*-purin-9-yl)-2,3-dihydroxy-*N*-methylbicyclo[3.1.0]hexane-1-carboxamide (34)—

Compound **34** (68%) was prepared from compound **44** following the same method as used for compound **27**. ¹H NMR (CD₃OD) δ 8.13 (s, 1H), 7.74-7.66 (m, 7H), 7.49-7.45 (m, 2H), 7.40-7.26 (m, 4H), 5.07 (d, *J* = 5.6 Hz, 1H), 4.9 (s, 1H), 4.60 (br s, 2H), 4.05 (d, *J* = 6.4 Hz, 1H), 2.85 (s, 3H), 2.14-2.11 (m, 1H), 1.89 (t, *J* = 4.8 Hz, 1H), 1.42-1.40 (m, 1H). HRMS calculated for C₃₄H₃₀ClN₆O₃ (M + H)⁺: 605.2068; found 605.2083.

(1*S*,2*R*,3*S*,4*R*,5*S*)-4-(6-(3-Chlorobenzylamino)-2-(pyren-1-ylethynyl)-9*H*-purin-9-yl)-2,3-dihydroxy-*N*-methylbicyclo[3.1.0]hexane-1-carboxamide (35)—

Compound **35** (91%) was prepared from compound **44** following the same method as used for compound **33**. ¹H NMR (CD₃OD) δ 8.71 (d, *J* = 9.2 Hz, 1H), 8.26-8.23 (m, 4H), 8.16-8.13 (m, 2H), 8.08-8.03 (m, 3H), 7.54 (s, 1H), 7.43 (d, *J* = 7.6 Hz, 1H), 7.34 (t, *J* = 8.0 Hz, 1H), 7.27 (d, *J* = 8.0 Hz, 1H), 5.06 (d, *J* = 6.4 Hz, 1H), 4.83 (s, 1H), 4.04 (d, *J* = 6.4 Hz, 1H), 2.81 (s, 3H), 2.10-2.07 (m, 1H), 1.89 (t, *J* = 4.8 Hz, 1H), 1.41-1.37 (m, 1H). HRMS calculated for C₃₈H₃₀ClN₆O₃ (M + H)⁺: 653.2068; found 653.2078.

(1*S*,2*R*,3*S*,4*R*,5*S*)-4-(6-(3-Chlorobenzylamino)-2-(pyren-4-ylethynyl)-9*H*-purin-9-yl)-2,3-dihydroxy-*N*-methylbicyclo[3.1.0]hexane-1-carboxamide (36)—

Compound **36** (69%) was prepared from compound **44** following the same method as used for compound **33**. ¹H NMR (CD₃OD) δ 8.82 (d, *J* = 7.6 Hz, 1H), 8.51 (s, 1H), 8.29-8.21 (m, 3H), 8.16-8.12 (m, 4H), 8.04 (t, *J* = 7.6 Hz, 1H), 7.54 (s, 1H), 7.43 (d, *J* = 7.6 Hz, 1H), 7.35 (t, *J* = 8.0 Hz, 1H), 7.28 (d, *J* = 8.4 Hz, 1H), 5.1 (d, *J* = 6.0 Hz, 1H), 4.06 (d, *J* = 6.0 Hz, 1H), 2.80 (s, 3H), 2.18-2.09 (m, 1H), 1.89 (t, *J* = 4.8 Hz, 1H), 1.42-1.39 (m, 1H). HRMS calculated for C₃₈H₃₀ClN₆O₃ (M + H)⁺: 653.2068; found 653.2056.

(1*S*,2*R*,3*S*,4*R*,5*S*)-Ethyl-(2,3-*O*-isopropylidene)-4-(2-iodo-6-(methylamino)-9*H*-purin-9-yl)bicyclo[3.1.0]hexane-1-carboxylate (41)—

Methylamine hydrochloride (0.353g, 5.23 mmol) and triethylamine (1.4 mL, 16.6 mmol) was added to a solution of compound **40** (0.528g, 1.04 mmol) in anhydrous methanol (15 mL) and stirred at room temperature overnight. Solvent was evaporated under vacuum, and the residue was purified on flash silica gel column chromatography (hexane:ethylacetate=1:1) to give compound **41** (0.470 g, 94%) as a foamy solid. ¹H NMR (CD₃OD) δ 7.94 (s, 1H), 5.83 (d, *J* = 7.2 Hz, 1H), 4.94 (s, 1H), 4.80 (d, *J* = 6.0 Hz, 1H), 4.33-4.27 (m, 2H), 3.05 (br s, 3H), 2.25-2.21 (m, 1H), 1.65-1.61 (m, 1H), 1.53-1.49 (m, 4H), 1.34 (t, *J* = 7.2 Hz, 3H), 1.29 (s, 3H). HRMS calculated for C₁₈H₂₃IN₅O₄ (M + H)⁺: 500.1072; found 500.1075.

(1*S*,2*R*,3*S*,4*R*,5*S*)-(2,3-*O*-Isopropylidene)-4-(2-iodo-6-(methylamino)-9*H*-purin-9-yl)-*N*-methylbicyclo[3.1.0]hexane-1-carboxamide (43)—

40% Methylamine solution (10 mL) was added to a solution of compound **41** (0.470 g, 0.94 mmol) in methanol (15 mL) and stirred at room temperature for 48 h. Solvent was evaporated under vacuum, and the residue was purified on flash silica gel column chromatography (CH₂Cl₂:MeOH=40:1) to give compound **43** (0.360 g, 79%) as a syrup. ¹H NMR (CD₃OD) δ 7.95 (s, 1H), 5.72 (d, *J* = 7.2 Hz, 1H), 4.93 (s, 1H), 4.84 (d, *J* = 7.2 Hz, 1H), 3.05 (br s, 3H), 2.90 (s, 3H), 2.17-2.11 (m, 1H), 1.54-1.49 (m, 4H), 1.39 (t, *J* = 5.2 Hz, 1H), 1.30 (s, 3H). HRMS calculated for C₁₇H₂₂IN₆O₃ (M + H)⁺: 485.0798; found 485.0803.

Pharmacological characterization

The nucleoside derivatives, dissolved as stock solutions in DMSO (5 mM) and stored frozen, were evaluated in binding²⁹⁻³¹ and a functional assay³⁴ at the A₃AR, binding assays at the A₁AR and A_{2A}AR, and a functional assay at the hA₃AR (details in Supporting Information). Use of heterologously expressed mouse ARs was as reported.^{33b,49} Protein

content was determined⁴⁸ and IC₅₀ values in binding inhibition transformed to K_i values⁵¹ as reported.

Molecular modeling

The Homology Model module of MOE was utilized to build a new molecular model of the hA₃AR (details in Supporting Information). The recently reported model of the complex of the nonselective AR agonist **59** docked to the crystal structure of the A_{2A}AR was used as a template for modeling of the A₃AR.^{25,51} The sequence alignment of the A_{2A} and A₃ARs was performed with MOE, taking into account positions of highly conserved amino acid residues. The position of full agonist **59** inside the A_{2A}AR was taken into account during the modeling. In the resulting initial homology model of the A₃AR (prior to movement of TM2), the complex 5',2,*N*⁶ trisubstituted agonist **59** used to crystallize the A_{2A}AR was removed and the simpler 5'-uronamide **58** docked inside the receptor. The Glide program of the Schrodinger package⁵² was used to dock the other agonists to the A₃AR model obtained. The receptor grid generation was performed for the box with a center in the centroid of **58** in its initial position. The size of the box was determined automatically. The extra precision mode (XP) of Glide was used for the docking. The binding site was defined as **58** and all amino acid residues located within 5 Å from **58**. All A₃AR residues located within 2 Å from the binding site were used as a shell. The following parameters of energy minimization were used: OPLS2005 force field, water was used as an implicit solvent, a maximum of 5000 iterations of the Polak-Ribier conjugate gradient minimization method was used with a convergence threshold of 0.01 kJ·mol⁻¹·Å⁻¹. Another reference nucleoside **58** was also docked in this hA₃AR homology model.

Hybrid A₃AR models involving movement of TM2, as explained above, were utilized to study the binding mode of analogue **34** and all other novel analogues in Table 1 using InducedFit docking implemented in the Schrödinger package. The grid generation was performed for a cubic box with sides of 26 Å and having a center in the centroid of the agonist molecules. The default values were used for other parameters.

Supplementary Material

Refer to Web version on PubMed Central for supplementary material.

Acknowledgments

We thank Dr. John Lloyd and Dr. Noel Whittaker (NIDDK) for mass spectral determinations. This research was supported by the Intramural Research Program of the NIH, National Institute of Diabetes and Digestive and Kidney Diseases and by NIH R01 HL077707.

Abbreviations

AR	adenosine receptor
cAMP	adenosine 3',5'-cyclic phosphate
CHO	Chinese hamster ovary
Cl-IB-MECA	2-chloro- <i>N</i> ⁶ -(3-iodobenzyl)-5'- <i>N</i> -methylcarboxamidoadenosine
DIPEA	diisopropylethylamine
DCM	dichloromethane
DMF	<i>N,N</i> -dimethylformamide

DMEM	Dulbecco's modified Eagle's medium
EDTA	ethylenediaminetetraacetic acid
EL	extracellular loop
GPCR	G protein-coupled receptor
HEK	human embryonic kidney
I-AB-MECA	N^6 -(4-amino-3-iodobenzyl)adenosine-5'- N -methyl-uronamide
IFD	Induced Fit docking
NECA	5'- N -ethylcarboxamidoadenosine
HEPES	4-(2-hydroxyethyl)-1-piperazineethanesulfonic acid
HRMS	high resolution mass spectroscopy
NMR	nuclear magnetic resonance
R-PIA	N^6 -R-phenylisopropyladenosine
TEA	triethylamine
TLC	thin layer chromatography
TM	transmembrane domain

References

1. a) Cheong SL, Federico S, Venkatesan G, Mandel AL, Shao YM, Moro S, Spalluto G, Pastorin G. The A₃ adenosine receptor as multifaceted therapeutic target: pharmacology, medicinal chemistry, and in silico approaches. *Med Res Rev*. 2012 in press. 10.1002/med.20254b) Jacobson KA, Balasubramanian R, DeFlorian F, Gao ZG. G protein-coupled adenosine (P1) and P2Y receptors. *Purinergic Signal*. 2012 in press. 10.1007/s11302-012-9294-7.
2. Fishman P, Jacobson KA, Ochaion A, Cohen S, Bar-Yehuda S. The anti-cancer effect of A₃ adenosine receptor agonists: A novel, targeted therapy. *Immun Endoc Metab Agents in Med Chem*. 2007; 7:298–303.
3. Silverman MH, Strand V, Markovits D, Nahir M, Reitlat T, Molad Y, Rosner I, Rozenbaum M, Mader R, Adawi M, Caspi D, Tishler M, Langevitz P, Rubinow A, Friedman J, Green L, Tanay A, Ochaion A, Cohen S, Kerns WD, Cohn I, Fishman-Furman S, Farbstein M, Bar-Yehuda S, Fishman P. Clinical evidence for utilization of the A₃ adenosine receptor as a target to treat rheumatoid arthritis: Data from a phase II clinical trial. *J Rheumatol*. 2008; 35:41–48. [PubMed: 18050382]
4. Gessi S, Merighi S, Varani K, Cattabriga E, Benini A, Mirandola P, Leung E, MacLennan S, Feo C, Baraldi S, Borea PA. Adenosine receptors in colon carcinoma tissues colon tumoral cell lines: focus on the A₃ adenosine subtype. *J Cell Physiol*. 2007; 211:826–836. [PubMed: 17348028]
5. Zheng J, Wang R, Zambraski E, Wu D, Jacobson KA, Liang BT. A novel protective action of adenosine A₃ receptors: Attenuation of skeletal muscle ischemia and reperfusion injury. *Am J Physiol, Heart and Circ Physiol*. 2007; 293:3685–3691.
6. Wan TC, Ge ZD, Tampo A, Mio Y, Bienengraeber MW, Tracey WR, Gross GJ, Kwok WM, Auchampach JA. The A₃ adenosine receptor agonist CP-532,903 [N^6 -(2,5-dichlorobenzyl)-3'-aminoadenosine-5'- N -methylcarboxamide] protects against myocardial ischemia/reperfusion injury via the sarcolemmal ATP-sensitive potassium channel. *J Pharmacol Exp Ther*. 2008; 324:234–243. [PubMed: 17906066]
7. Guzman J, Yu JG, Suntres Z, Bozarov A, Cooke H, Javed N, Auer H, Palatini J, Hassanain HH, Cardounel AJ, Javed A, Grants I, Wunderlich JE, Christofi FL. ADOA3R as a therapeutic target in experimental colitis: Proof by validated high-density oligonucleotide microarray analysis. *Inflamm Bowel Dis*. 2006; 12:766–789. [PubMed: 16917233]

8. (a) Fishman P, Bar-Yehuda S, Liang BT, Jacobson KA. Pharmacological and therapeutic effects of A₃ adenosine receptor (A₃AR) agonists. *Drug Disc Today*. 2012; 17:359–366. (b) Gessi S, Merighi S, Varani K, Leung E, MacLennan S, Borea PA. The A₃ adenosine receptor: An enigmatic player in cell biology. *Pharmacology & Therapeutics*. 2008; 117:123–140. [PubMed: 18029023]
9. Yamano K, Inoue M, Masaki S, Saki M, Ichimura M, Satoh M. Generation of adenosine A₃ receptor functionally humanized mice for the evaluation of the human antagonists. *Biochem Pharmacol*. 2006; 71:294–306. [PubMed: 16300745]
10. Yang H, Avila MY, Peterson-Yantorno K, Coca-Prados M, Stone RA, Jacobson KA, Civan MM. The cross-species A₃ adenosine-receptor antagonist MRS 1292 inhibits adenosine-triggered human nonpigmented ciliary epithelial cell fluid release and reduces mouse intraocular pressure. *Current Eye Res*. 2005; 30:747–754.
11. Hua X, Chason KD, Fredholm BB, Deshpande DA, Penn RB, Tilley SL. Adenosine induces airway hyperresponsiveness through activation of A₃ receptors on mast cells. *J Allergy Clin Immunol*. 2008; 122:107–113. [PubMed: 18472152]
12. Bulger EM, Tower CM, Warner KJ, Garland T, Cuschieri J, Rizoli S, Rhind S, Junger WG. Increased neutrophil adenosine A₃ receptor expression is associated with hemorrhagic shock and injury severity in trauma patients. *Shock*. 2011; 36:435–439. [PubMed: 21841534]
13. (a) Gao ZG, Kim SK, Biadatti T, Chen W, Lee K, Barak D, Kim SG, Johnson CR, Jacobson KA. Structural determinants of A₃ adenosine receptor activation: Nucleoside ligands at the agonist/antagonist boundary. *J Med Chem*. 2002; 45:4471–4484. [PubMed: 12238926] (b) Jeong LS, Lee HW, Jacobson KA, Kim HO, Shin DH, Lee JA, Gao ZG, Lu C, Duong HT, Gunaga P, Lee SK, Jin DZ, Chun MW, Moon HR. Structure-activity relationships of 2-chloro-N⁶-substituted-4'-thioadenosine-5'-uronamides as highly potent and selective agonists at the human A₃ adenosine receptor. *J Med Chem*. 2006; 49:273–281. [PubMed: 16392812] (c) Elzein E, Palle V, Wu Y, Maa T, Zeng D, Zablocki J. 2-Pyrazolyl-N⁶-substituted adenosine derivatives as high affinity and selective adenosine A₃ receptor agonists. *J Med Chem*. 2004; 47:4766–4773. [PubMed: 15341491] (d) DeNinno MP, Masamune H, Chenard LK, DiRico KJ, Eller C, Etienne JB, Tickner JE, Kennedy SP, Knight DR, Kong J, Oleynek JJ, Tracey WR, Hill RJ. The synthesis of highly potent, selective, and water-soluble agonists at the human adenosine A₃ receptor. *Bioorg Med Chem Lett*. 2006; 16:2525–2527. [PubMed: 16464581] (e) Cosyn L, Palaniappan KK, Kim SK, Duong HT, Gao ZG, Jacobson KA, Van Calenbergh S. 2-Triazole-substituted adenosines: A new class of selective A₃ adenosine receptor agonists, partial agonists, and antagonists. *J Med Chem*. 2006; 49:7373–7383. [PubMed: 17149867]
14. Jacobson KA, Ji X-d, Li AH, Melman N, Siddiqui MA, Shin KJ, Marquez VE, Ravi RG. Methanocarba analogues of purine nucleosides as potent and selective adenosine receptor agonists. *J Med Chem*. 2000; 43:2196–2203. [PubMed: 10841798]
15. Lee K, Ravi RG, Ji X-d, Marquez VE, Jacobson KA. Ring-constrained (N)methanocarba-nucleosides as adenosine receptor agonists: Independent 5'-uronamide and 2'-deoxy modifications. *Bioorg Med Chem Lett*. 2001; 11:1333–1337. [PubMed: 11392549]
16. Tchilibon S, Joshi BV, Kim SK, Duong HT, Gao ZG, Jacobson KA. Methanocarba 2,N⁶-disubstituted adenine nucleosides as highly potent and selective A₃ adenosine receptor agonists. *J Med Chem*. 2005; 48:1745–1758. [PubMed: 15771421]
17. Ochaion A, Bar-Yehuda S, Cohen S, Amital H, Jacobson KA, Joshi BV, Gao ZG, Barer F, Patoka R, Del Valle L, Perez-Liz G, Fishman P. The A₃ adenosine receptor agonist CF502 inhibits the PI3K, PKB/Akt and NF-κB signaling pathway in synoviocytes from rheumatoid arthritis patients and in adjuvant induced arthritis rats. *Biochem Pharmacol*. 2008; 76:482–494. [PubMed: 18602896]
18. Matot I, Weinger CF, Zeira E, Galun E, Joshi BV, Jacobson KA. A₃ Adenosine receptors and mitogen activated protein kinases in lung injury following in-vivo reperfusion. *Critical Care*. 2006; 10:R65. [PubMed: 16623960]
19. Chen Z, Janes K, Chen C, Doyle T, Tosh DK, Jacobson KA, Salvemini D. Controlling murine and rat chronic pain through A₃ adenosine receptor activation. *FASEB J*. 2012 in press. 10.1096/fj.11-201541
20. (a) Volpini R, Dal Ben D, Lambertucci C, Taffi S, Vittori S, Klotz KN, Cristalli GJ. N⁶-Methoxy-2-alkynyladenosine derivatives as highly potent and selective ligands at the human A₃

- adenosine receptor. *J Med Chem.* 2007; 50:1222–1230. [PubMed: 17309246] (b) Cristalli G, Lambertucci C, Marucci G, Volpini R, Dal Ben D. A_{2A} Adenosine receptor and its modulators: Overview on a druggable GPCR and on structure-activity relationship analysis and binding requirements of agonists and antagonists. *Curr Pharm Des.* 2008; 14:1525–1552. [PubMed: 18537675]
21. Melman A, Gao ZG, Kumar D, Wan TC, Gizewski E, Auchampach JA, Jacobson KA. Design of (N)-methanocarba adenosine 5'-uronamides as species-independent A₃ receptor-selective agonists. *Bioorg Med Chem Lett.* 2008; 18:2813–2819. [PubMed: 18424135]
 22. Dooley MJ, Quinn RJ. The three binding domain model of adenosine receptors: molecular modeling aspects. *J Med Chem.* 1992; 35:211–217. [PubMed: 1732538]
 23. (a) Volpini R, Buccioni M, Dal Ben D, Lambertucci C, Lammi C, Marucci G, Ramadori AT, Klotz KN, Cristalli G. Synthesis and biological evaluation of 2-alkynyl-N⁶-methyl-5'-N-methylcarboxamidoadenosine derivatives as potent and highly selective agonists for the human adenosine A₃ receptor. *J Med Chem.* 2009; 52:7897–7900. [PubMed: 19839592] (b) Dal Ben D, Lambertucci C, Lammi C, Marucci G, Thomas A, Volpini R, Cristalli G. Molecular modeling study on potent and selective adenosine A₃ receptor agonists. *Bioorg Med Chem.* 2010; 18:7923–7930. [PubMed: 20943397]
 24. Sevillano, LG.; McGuigan, C.; Davies, RH. Compounds useful as A₃ adenosine receptor agonists. U.S. Patent 7,414,036 B2. 2008.
 25. Xu F, Wu H, Katritch V, Han GW, Jacobson KA, Gao ZG, Cherezov V, Stevens RC. Structure of an agonist-bound human A_{2A} adenosine receptor. *Science.* 2011; 332:322–327. [PubMed: 21393508]
 26. Congreve M, Langmead CJ, Mason JS, Marshall FH. Progress in structure based drug design for G protein-coupled receptors. *J Med Chem.* 2011; 54:4283–4311. [PubMed: 21615150]
 27. Chinchilla R, Nájera C. The Sonogashira reaction: A booming methodology in synthetic organic chemistry. *Chem Rev.* 2007; 107:874–922. [PubMed: 17305399]
 28. Tosh DK, Chinn M, Ivanov AA, Klutz AM, Gao ZG, Jacobson KA. Functionalized congeners of A₃ adenosine receptor-selective nucleosides containing a bicyclo[3.1.0]hexane ring system. *J Med Chem.* 2009; 52:7580–7592. [PubMed: 19499950]
 29. Schwabe U, Trost T. Characterization of adenosine receptors in rat brain by (–)-[³H]N⁶-phenylisopropyladenosine. *Naunyn Schmiedebergs Arch Pharmacol.* 1989; 313:179–187. [PubMed: 6253840]
 30. Jarvis MF, Schutz R, Hutchison AJ, Do E, Sills MA, Williams M. [³H]CGS 21680 an A₂ selective adenosine receptor agonist directly labels A₂ receptors in rat brain tissue. *J Pharmacol Exp Ther.* 1989; 251:888–893. [PubMed: 2600819]
 31. Olah ME, Gallo-Rodriguez C, Jacobson KA, Stiles GL. ¹²⁵I-4-Aminobenzyl-5'-N-methylcarboxamidoadenosine, a high affinity radioligand for the rat A₃ adenosine receptor. *Mol Pharmacol.* 1994; 45:978–982. [PubMed: 8190112]
 32. Englert M, Qwitterer U, Klotz KN. Effector coupling of stably transfected human A₃ adenosine receptors in CHO cells. *Biochem Pharmacol.* 2002; 64:61–65. [PubMed: 12106606]
 33. (a) Jacobson KA, Park KS, Jiang J-l, Kim YC, Olah ME, Stiles GL, Ji Xd. Pharmacological characterization of novel A₃ adenosine receptor-selective antagonists. *Neuropharmacology.* 1997; 36:1157–1165. [PubMed: 9364471] (b) Ge ZD, Peart JN, Kreckler LM, Wan TC, Jacobson MA, Gross GJ, Auchampach JA. Cl-IB-MECA [2-chloro-N⁶-(3-iodobenzyl)adenosine-5'-N-methylcarboxamide] reduces ischemia/reperfusion injury in mice by activating the A₃ adenosine receptor. *J Pharmacol Exp Ther.* 2006; 319:1200–1210. [PubMed: 16985166]
 34. Nordstedt C, Fredholm BB. A modification of a protein-binding method for rapid quantification of cAMP in cell-culture supernatants and body fluid. *Anal Biochem.* 1990; 189:231–234. [PubMed: 2177960]
 35. Sherman W, Day T, Jacobson MP, Friesner RA, Farid R. Novel Procedure for Modeling Ligand/Receptor Induced Fit Effects. *J Med Chem.* 2006; 49:534–553. [PubMed: 16420040]
 36. Ivanov AA, Barak D, Jacobson KA. Evaluation of homology modeling of GPCRs in light of the A_{2A} adenosine receptor crystallographic structure. *J Med Chem.* 2009; 52:3284–3292. [PubMed: 19402631]

37. Jaakola VP, Lane JR, Lin JY, Katritch V, IJzerman AP, Stevens RC. Ligand binding and subtype selectivity of the human A_{2A} adenosine receptor: identification and characterization of essential amino acid residues. *J Biol Chem*. 2010; 285:13032–13044. [PubMed: 20147292]
38. Costanzi S, Ivanov AA, Tikhonova IG, Jacobson KA. Structure and function of G protein-coupled receptors studied using sequence analysis, molecular modeling and receptor engineering: adenosine receptors. *Front Drug Des Discov*. 2007; 3:63–79.
39. O'Malley MA, Naranjo AN, Lazarova T, Robinson AS. Analysis of adenosine A_{2A} receptor stability: Effects of ligands and disulfide bonds. *Biochemistry*. 2010; 49:9181–9189. [PubMed: 20853839]
40. Rasmussen SGF, DeVree BT, Zou Y, Kruse AC, Chung KY, Kobilka TS, Thian FS, Chae PS, Pardon E, Calinski D, Mathiesen JM, Shah STA, Lyons JA, Caffrey M, Gellman SH, Steyaert J, Skinotits G, Weis WI, Sunihara RK, Kobilka BK. Crystal structure of the β₂ adrenergic receptor–Gs protein complex. *Nature*. 2011; 477:549–555. [PubMed: 21772288]
41. Scheerer P, Park JH, Hildebrand PW, Kim YJ, Krauss N, Choe HW, Hofmann KP, Ernst OP. Crystal structure of opsin in its G-protein-interacting conformation. *Nature*. 2008; 455:497–502. [PubMed: 18818650]
42. Baraldi PG, Cacciari B, Pineda de las Infantas MJ, Romagnoli R, Spalluto G, Volpini R, Costanzi S, Vittori S, Cristalli G, Melman N, Park KS, Ji X-d, Jacobson KA. Synthesis and biological activity of a new series of N⁶-arylcarbamoyl-, 2-(ar)alkynyl-N⁶-arylcarbamoyl, and N⁶-carboxamido- derivatives of adenosine-5'-N-ethyluronamide (NECA) as A₁ and A₃ adenosine receptor agonists. *J Med Chem*. 1998; 41:3174–3185. [PubMed: 9703463]
43. Bickerton GR, Paolini GV, Besnard J, Muresan S, Hopkins AL. Quantifying the chemical beauty of drugs. *Nature Chem*. 2012; 4:90–98. [PubMed: 22270643]
44. Deflorian F, Kumar TS, Phan K, Gao ZG, Xu F, Wu H, Katritch V, Stevens RC, Jacobson KA. Evaluation of molecular modeling of agonist binding in light of the crystallographic structure of the agonist-bound A_{2A} adenosine receptor. *J Med Chem*. 2012; 55:538–552. [PubMed: 22104008]
45. Moro S, Deflorian F, Bacilieri M, Spalluto G. Ligand-based homology modeling as attractive tool to inspect GPCR structural plasticity. *Curr Pharm Des*. 2006; 12:2175–2185. [PubMed: 16796562]
46. Hardegger LA, Kuhn B, Spinnler B, Anselm L, Ecabert R, Stihle M, Gsell B, Thoma R, Diez J, Benz J, Plancher JM, Hartmann G, Banner DW, Haap W, Diederich F. Systematic investigation of halogen bonding in protein-ligand interactions. *Angew Chem Int Engl Ed*. 2011; 50:314–318.
47. Kiesewetter DO, Lang L, Ma Y, Bhattacharjee AK, Gao ZG, Joshi BV, Melman A, Castro S, Jacobson KA. Synthesis and characterization of [⁷⁶Br]-labeled high affinity A₃ adenosine receptor ligands for positron emission tomography. *Nucl Med Biol*. 2009; 36:3–10. [PubMed: 19181263]
48. Bradford MM. A rapid and sensitive method for the quantitation of microgram quantities of protein utilizing the principle of protein-dye binding. *Anal Biochem*. 1976; 72:248–254. [PubMed: 942051]
49. Kreckler LM, Wan TC, Ge ZD, Auchampach JA. Adenosine inhibits tumor necrosis factor-α release from mouse peritoneal macrophages via A_{2A} and A_{2B} but not the A₃ adenosine receptors. *J Pharmacol Exp Ther*. 2006; 317:172–180. [PubMed: 16339914]
50. Cheng YC, Prusoff WH. Relationship between inhibition constant (K₁) and concentration of inhibitor which causes 50 percent inhibition (I₅₀) of an enzymatic-reaction. *Biochem Pharmacol*. 1973; 22:3099–3108. [PubMed: 4202581]
51. Tosh DK, Phan K, Deflorian F, Wei Q, Gao ZG, Jacobson KA. Truncated (N)-Methanocarba Nucleosides as A₁ Adenosine Receptor Agonists and Partial Agonists: Overcoming Lack of a Recognition Element. *ACS Med Chem Lett*. 2011; 2:626–631. [PubMed: 21858244]
52. Mohamadi FN, Richards GJ, Guida WC, Liskamp R, Lipton M, Caufield C, Chang G, Hendrickson T, Still WC. MacroModel an integrated software system for modeling organic and bioorganic molecules using molecular mechanics. *J Comput Chem*. 1990; 11:440–467.

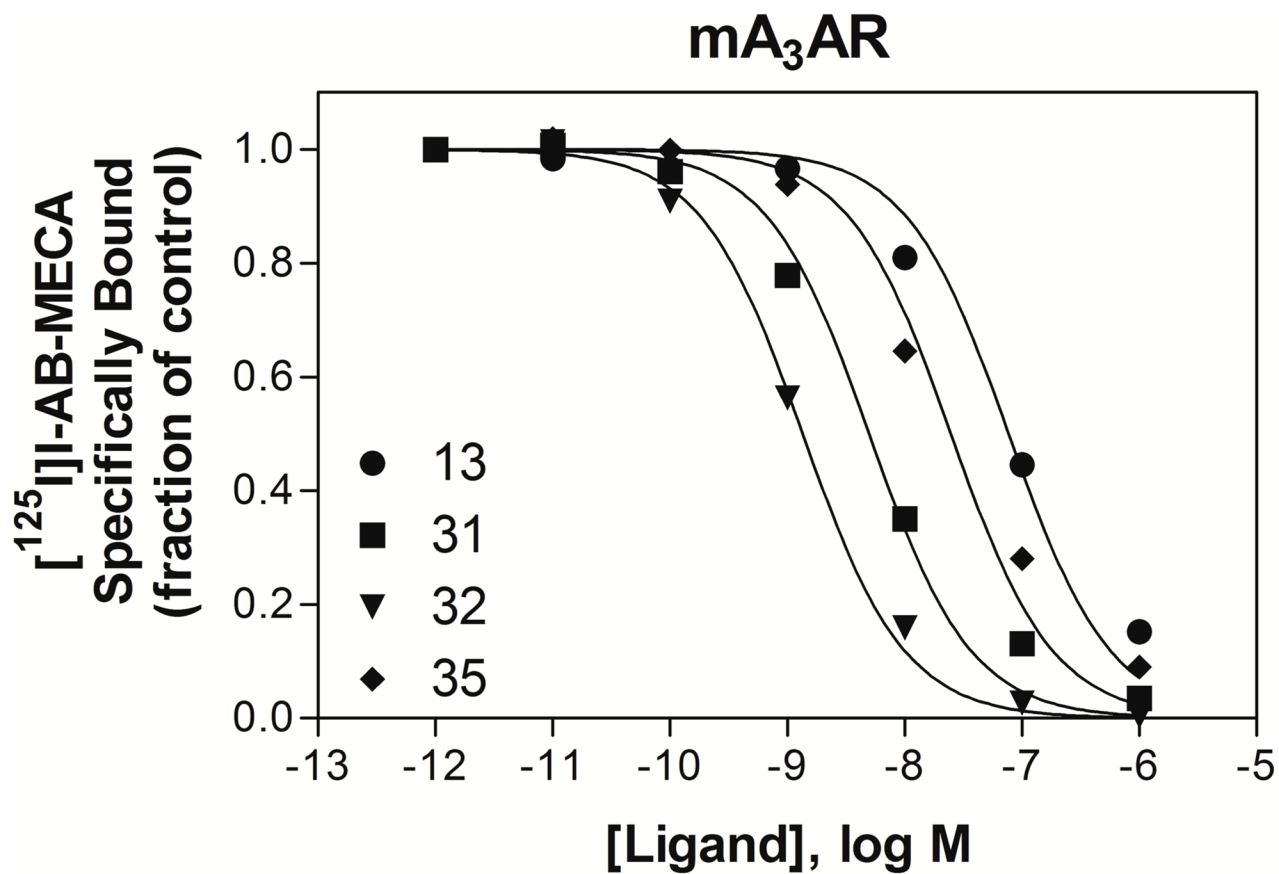


Figure 1. Inhibition of binding of the radioligand [¹²⁵I]54 (0.3 nM) at the mA₃AR by compounds 13, 31, 32 and 34. K_i values are found in Table 2.

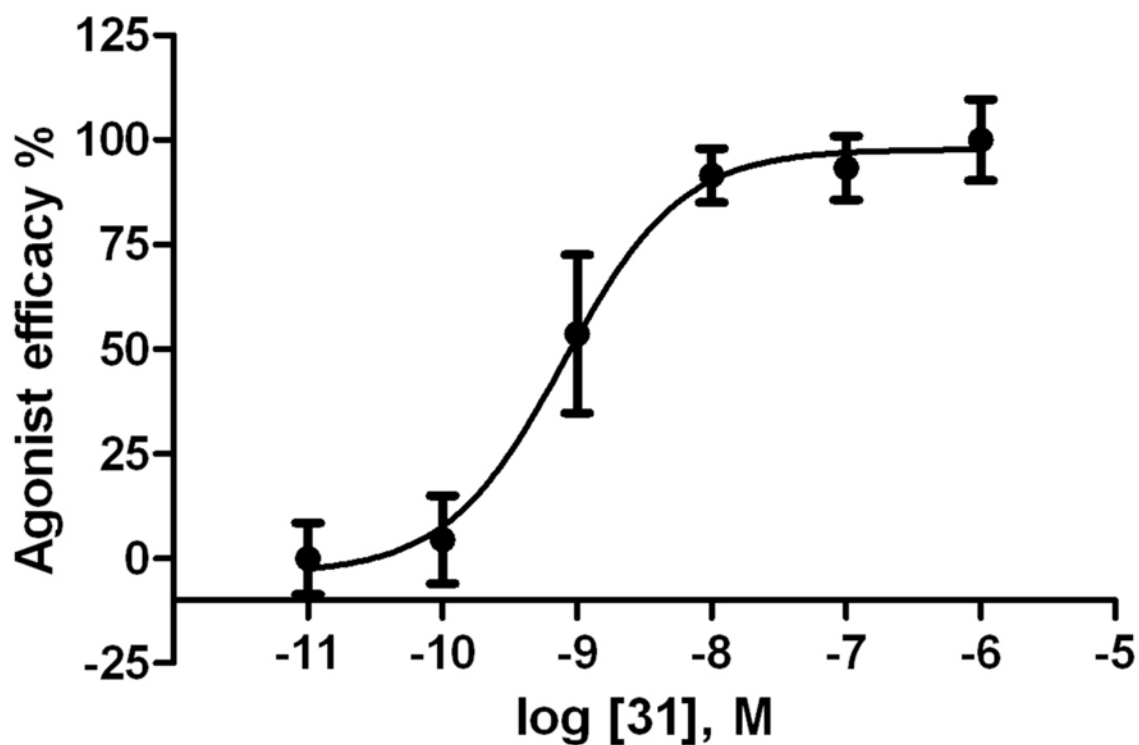


Figure 2. Functional agonism by the tested in an assay of adenylate cyclase in membranes of CHO cells expressing the hA₃AR. Activity of the 2-(3,4-difluorophenylethynyl)-N⁶-3-chlorobenzyl-5'-N-methyluronamide-(N)-methanocarba analogue **31** (EC₅₀ value 1.2±0.7 nM). The full agonist 5'-N-ethyluronamidoadenosine **48** was included for comparison (representing 100% efficacy). The experiment was repeated three times, and the average is shown.

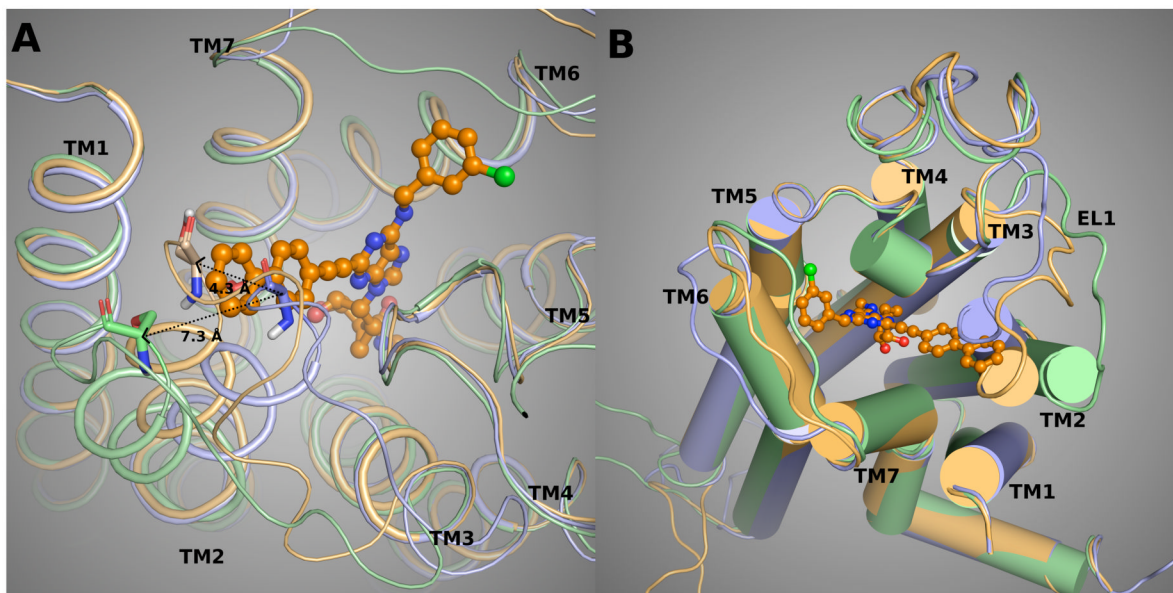
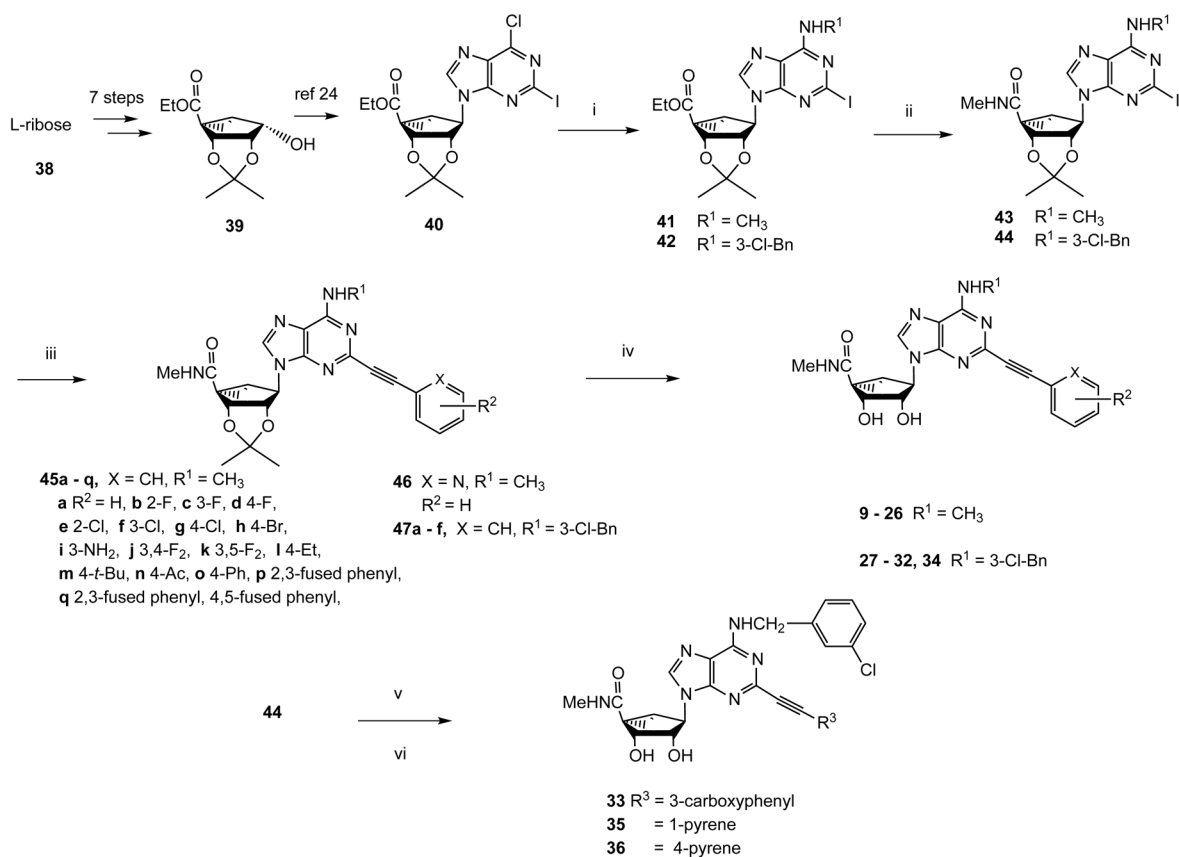
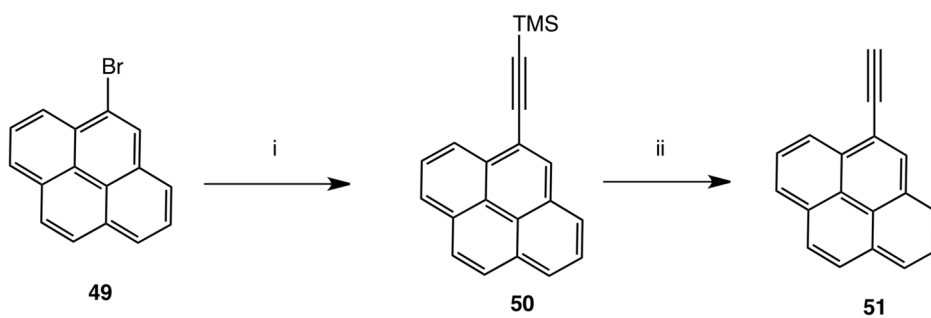


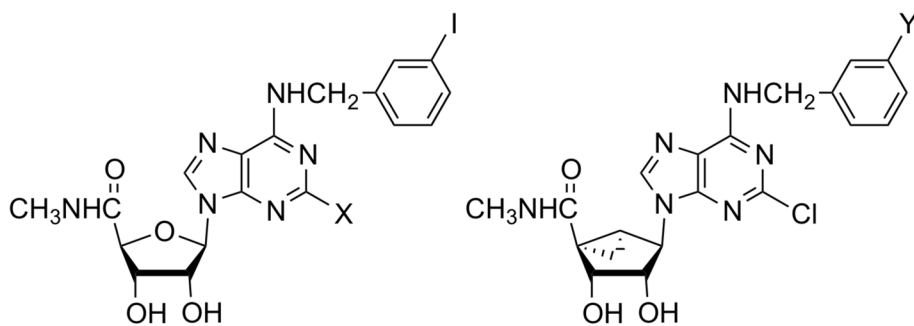
Figure 3. The binding mode (two different views with **A.** wire helices and **B.** tube helices) of linearly extended N^6 -3-chlorobenzyl analogue **34** obtained after IFD to the A_3 AR homology model. The template was built based on the crystal structure of an agonist-bound A_{2A} AR (purple helices)²⁵ and adjusted for movement of TM2 based on other templates (β_2 -adrenergic receptor, brown helices; opsin, green helices).^{40,41} The most successful template for TM2 was the structure of opsin.

**Scheme 1.**

Synthesis of (N)-methanocarba nucleoside analogues. R₁ = Me or 3-Cl-benzyl. Reagents: (i) MeNH₂ or 3-Cl-benzylamine, Et₃N, MeOH, rt; (ii) 40% MeNH₂, MeOH, rt; (iii) HC≡CAr, Pd(PPh₃)₂Cl₂, CuI, Et₃N, DMF, rt; (iv) 10% TFA, MeOH, 70°C; (v) 1-ethynylpyrene or 4-ethynylpyrene **51**, Pd(PPh₃)₂Cl₂, CuI, Et₃N, DMF, rt; (vi) HCl, 1 N, dioxane, 60°C.

**Scheme 2.**

Synthesis of an intermediate arylalkynyl derivative. (i) HC≡C-TMS, Pd(PPh₃)₂Cl₂, CuI, Et₃N, DMF, rt; (ii) TBAF, THF.



1 X = H IB-MECA

2 X = Cl Cl-IB-MECA

3 Y = 3-Cl MRS3558

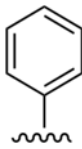
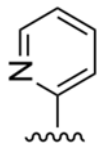
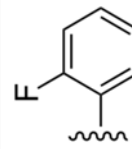
4 Y = 3-I MRS1898

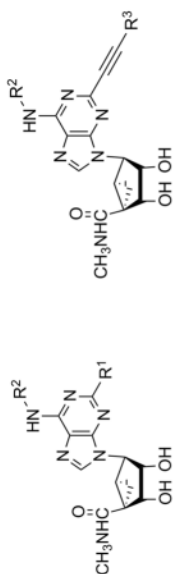
Chart 1.

Derivatives of adenosine as A₃AR-selective agonists in the ribose (**1**, **2**) and (N)-methanocarba (**3**, **4**) series.

Table 1

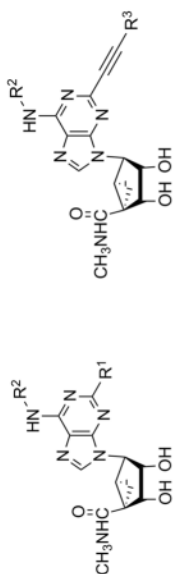
Binding affinity of a series of (N)-methanocarba adenosine derivatives at three subtypes of hARs and the functional efficacy at the hA₃AR.

Compd	Structure		Affinity (K _p , nM) or % inhibition ^a				% Efficacy ^b	
	R ¹ or R ³	R ²	hA ₁	hA _{2A}	hA ₃	hA ₃	hA ₃	
3c	Cl	3-Cl-Bn	260±60	2300±100	0.29±0.04	103±7		
4c,d	Cl	3-I-Bn	136±22	784±97	1.5±0.2	100		
5c	H	3-I-Bn	700±270	6200±100	2.4±0.5	100		
6d	C≡CH	3-Cl-Bn	174±23	(48%)	1.30±0.38	ND		
7d	C≡C(CH ₂) ₂ CH ₃	3-Cl-Bn	1040±83	(80%)	0.82±0.20	ND		
8c,d	Cl	CH ₃	2100±1700	(6%)	2.2±0.6	ND		
9		CH ₃	(13%±6%)	(14%±7%)	0.85±0.22	89.3±7.7		
10		CH ₃	(11%±4%)	(13%±4%)	1.01±0.36	86.8±9.2		
11		CH ₃	(21%±4%)	(17%±2%)	0.97±0.38	97.7±9.1		

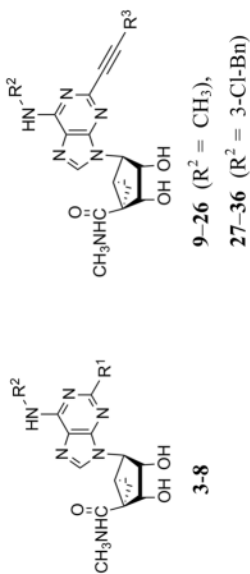


3-8

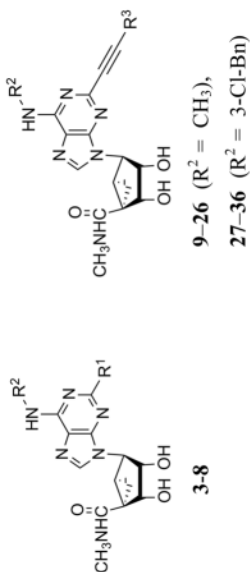
9-26 (R² = CH₃),
27-36 (R² = 3-Cl-Bn)



Compd	Structure		Affinity (K_i , nM) or % inhibition ^d				% Efficacy ^b	
	R ¹ or R ³	R ²	hA ₁	hA _{2A}	hA ₃	hA ₃	hA ₃	
12		CH ₃	(12% ± 2%)	(10% ± 5%)	0.97 ± 0.24	95.8 ± 6.7		
13		CH ₃	(21% ± 1%)	(19% ± 3%)	0.53 ± 0.09	80.3 ± 5.8		
14		CH ₃	(27% ± 7%)	(30% ± 5%)	0.58 ± 0.04	84.2 ± 6.2		
15		CH ₃	(10% ± 2%)	1270 ± 300	1.60 ± 0.60	90.9 ± 1.9		
16		CH ₃	(14% ± 1%)	(30% ± 1%)	1.22 ± 0.31	97.4 ± 9.1		
17		CH ₃	(13% ± 7%)	(26% ± 1%)	0.91 ± 0.06	97.5 ± 12.3		
18		CH ₃	(10% ± 5%)	(19% ± 14%)	1.07 ± 0.14	109 ± 4.1		



Compd	Structure		Affinity (K_i , nM) or % inhibition ^a				% Efficacy ^b	
	R ¹ or R ³	R ²	hA ₁	hA _{2A}	hA ₃	hA ₃	hA ₃	
19		CH ₃	(6%±3%)	(6%±6%)	1.65±0.08	108±1.9		
20		CH ₃	(8%±3%)	(47%±4%)	1.66±0.36	99.6±3.3		
21		CH ₃	(13%±3%)	(38%±5%)	3.78±1.16	110±4.9		
22		CH ₃	(23%±5%)	(7%±5%)	10.1±1.9	78.4±6.5		
23		CH ₃	(15%±7%)	5300±600	2.57±0.78	87.4±9.9		
24		CH ₃	(21%±6%)	(29%±8%)	3.10±1.26	110±2.9		
25		CH ₃	(25%±1%)	(34%±8%)	1.67±0.18	94.6±4.4		



Compd	Structure	Affinity (K_i , nM) or % inhibition ^a			% Efficacy ^b
		R ¹ or R ³	R ²	hA ₁ , hA _{2A} , hA ₃	
26			CH ₃	hA ₁ (15%±5%) hA _{2A} (52%±1%) hA ₃ 3.48±1.36	108±3.5
27			3-Cl-Bn	hA ₁ (20%±3%) hA _{2A} (27%±3%) hA ₃ 1.34±0.30	101±5.9
28			3-Cl-Bn	hA ₁ (20%±6%) hA _{2A} (42%±2%) hA ₃ 2.16±0.34	102±1.4
29			3-Cl-Bn	hA ₁ (19%±2%) hA _{2A} (52%±12%) hA ₃ 1.92±0.57	103±1.5
30			3-Cl-Bn	hA ₁ (4%±4%) hA _{2A} 1740±590 hA ₃ 4.45±1.39	91.5±11.4
31			3-Cl-Bn	hA ₁ (6%±4%) hA _{2A} (41%±10%) hA ₃ 3.49±1.84	95.7±6.4

Compd	Structure	Affinity (K _i , nM) or % inhibition ^d			% Efficacy ^b		
		R ¹ or R ³	R ²	hA ₁	hA _{2A}	hA ₃	
32		NH ₂	3-Cl-Bn	1520±300	(44%±4%)	2.27±0.70	76.6±13.1
33		CO ₂ H	3-Cl-Bn	(6%±5%)	(38%±5%)	6.75±2.78	86.7±5.4
34		Phenyl	3-Cl-Bn	(2%±2%)	(0%±0%)	3.06±1.35	89.0±4.5
35		Naphthalene	3-Cl-Bn	(8%±2%)	3110±530	68.3±12.5	77.8±11.6
36		Fluorene	3-Cl-Bn	(11±5%)	(4±3%)	660±170	97.1±3.3

9-26 (R² = CH₃),
27-36 (R² = 3-Cl-Bn)

3-8

^aAll experiments were done on CHO or HEK293 (A_{2A} only) cells stably expressing one of three subtypes of the four hARs. The binding affinity for A₁, A_{2A} and A₃ARs was expressed as K_i values (n = 3-5) and was determined by using agonist radioligands ([³H]N⁶-R-phenylisopropyladenosine **52** (R-PIA), [³H]2-[p-(2-carboxylethyl)phenyl-ethylamino]-5'-N-ethylcarboxamidoadenosine **53** (CGS21680), or [³H]N⁶-(4-amino-3-iodobenzyl)adenosine-5'-N-methyl-uronamide **54** (I-AB-MECA), respectively), unless noted.²⁹⁻³¹ A percent in parentheses refers to inhibition of radioligand binding at 10 μM (n = 3).

^b Unless noted, the efficacy at the hA₃AR was determined by inhibition of forskolin-stimulated cAMP production in AR-transfected CHO cells.³²⁻³⁴ At a concentration of 10 μM, in comparison to the maximal effect of 5'-N-ethylcarboxamidoadenosine **48** (=100%) at 10 μM. Data are expressed as mean±standard error (n = 3).

^c Values from Lee et al.; Tchilibon et al.^{15,16}

^d Values from Melman et al.²¹

ND, not determined.

Table 2

Binding affinity of a series of (N)-methanocarba adenosine derivatives at three subtypes of mARs.

Compd	Affinity (K_i , nM) or % inhibition ^a		
	mA ₁	mA _{2A}	mA ₃
3^b	15.3±5.8	10,400±1,700	1.49±0.46
4^b	7.32±1.5	5,350±860	0.80±0.14
6^b	45.6±7.9	(41% ^j)	0.85±0.08
7^b	1390±430	(42% ^j)	6.06±1.21
8^b	55.3±6.0	20,400±3,200	49.0±3.9
13	(29±2%)	(0%)	37.7±1.1
14	(55±5%)	(2±1%)	37.2±2.0
27	(50±5%)	(2±1%)	1.23±0.14
28	(65±3%)	(7±2%)	2.38±0.04
29	(51±12%)	(19±3%)	2.64±0.22
30	(35±3%)	(55%)	2.39±0.38
31	(14±3%)	(27±2%)	3.08±0.23
32	261±19	(5±2%)	0.82±0.06
33	(18±3%)	(22%)	3.66±0.25
34	(41±6%)	(6±1%)	10.8±0.93
35	(8±2%)	(64%)	47.6±4.6

^aCompetition radioligand binding assays using [¹²⁵I]54 (A₁ and A₃ARs) and [³H]53 (A_{2A}AR) were conducted with membranes prepared from HEK293 cells expressing recombinant mA₁, A_{2A}, or A₃ARs. The data (n = 3–4) are expressed as K_i values. A percent in parentheses refers to inhibition of radioligand binding at 10 μ M.

^bValues from Melman et al.²¹